Journal of Applied Physics PERSPECTIVE scitation.org/journal/jap

Next generation of nanozymes: A perspective of the challenges to match biological performance

Cite as: J. Appl. Phys. **130**, 190903 (2021); doi: 10.1063/5.0061499
Submitted: 27 June 2021 · Accepted: 9 October 2021 ·
Published Online: 15 November 2021

G. F. Goya,[1,2,a)] A. Mayoral,[2,3,4] E. Winkler,[5,6] R. D. Zysler,[5,6] C. Bagnato,[7] M. Raineri,[5] J. A. Fuentes-García,[2] and E. Lima, Jr.[5]

AFFILIATIONS

[1]Departamento de Física de la Materia Condensada, Facultad de Ciencias, Universidad de Zaragoza, 50009 Zaragoza, Spain
[2]Instituto de Nanociencia y Materiales de Aragón (INMA), CSIC-Universidad de Zaragoza, 50018 Zaragoza, Spain
[3]Advanced Microscopy Laboratory (LMA), University of Zaragoza, Zaragoza 50018, Spain
[4]Center for High-Resolution Electron Microscopy (C*h*EM), School of Physical Science and Technology (SPST), Shanghai Tech University, 393 Middle Huaxia Road, Pudong, Shanghai 201210, China
[5]Instituto de Nanociencia y Nanotecnología, CNEA-CONICET, San Carlos de Bariloche, Río Negro R8402AGP, Argentina
[6]Instituto Balseiro, Universidad Nacional de Cuyo, San Carlos de Bariloche, Río Negro, Argentina
[7]Instituto de Energía y Desarrollo Sustentable (IEDS), CNEA, Centro Atómico Bariloche, San Carlos de Bariloche, Rio Negro, Argentina

[a)]**Author to whom correspondence should be addressed:** goya@unizar.es

ABSTRACT

Nanomaterials with enzyme-like activity have been the spotlight of scientific and technological efforts to substitute natural enzymes, not only in biological research but also for industrial manufacturing, medicine, and environment healing. Notable advancements in this field along the last years relied on to the rational design of single-atom active sites, knowledge of the underlying atomic structure, and realistic *ab initio* theoretical models of the electronic configuration at the active site. Thus, it is plausible that a next generation of nanozymes still to come will show even improved catalytic efficiency and substrate specificity. However, the dynamic nature of the protein cage surrounding most active sites in biological enzymes adds a flexible functionality that possess a challenge for nanozyme's mimicking of their natural counterparts. We offer a perspective about where the main strategies to improve nanozymes are headed and identify some of the big challenges faced along the road to better performance. We also outline some of the most exciting bio-inspired ideas that could potentially change this field.

I. OVERVIEW AND CURRENT SITUATION IN THE FIELD OF NANOZYMES

Natural enzymes are those biomolecules that regulate the rates of biochemical reactions in living organisms, as an essential part of cell metabolic pathways. Enzymes have either extreme specificity to catalyze a reaction for a single molecule or flexibility for catalyzing a whole group of biochemical reactions. Several decades ago, researchers began to imagine different ways to exploit these properties of enzymes for industrial manufacturing activities including food, paper, and pharmaceutical sectors to face severe environmental degradation, energy impact, and resource depletion.[1] This new field, known as enzymatic biocatalysis, has allowed notable advancements in material-efficient and sustainable patterns of production and consumption.[2] However, natural enzymes lack enough availability for the large scales required for industrial applications. Additionally, natural enzymes are complex molecules evolutionary optimized to perform under physiological conditions, and this imposes strict limits to protect their catalytic activity (e.g., physiological pH and temperature values). Therefore, preserving the integrity of these biomolecules under the harsh conditions of industrial processes has been one of the many challenges of the biocatalysis field.[3]

The concept of artificial enzyme was introduced in the 1970s, after the first observation of increased deacetylation reaction rates up to 10^7 times by of metal groups.[4] This observation was followed by countless reports on enzyme-like activities involving inorganic materials[5,6] and the term "nanozyme" was coined to identify them as a synthetic counterpart of natural enzymes.[7] With the irruption of nanotechnology, nanomaterials were also confirmed to mimic several biological enzymes as a standalone inorganic system, with the pivotal report by Gao *et al.* showing the peroxidase-like activity of Fe_3O_4 nanoparticles.[8] Since then, multiple enzymatic-like activities have been reported including peroxidase,[9] catalase,[10] superoxide dismutase,[11] and phosphatase.[12] However, some authors have questioned the very concept of nanozyme, arguing the fundamental differences between enzymatic activity and oxidation chemistry, as distinct mechanisms behind the observed formation of hydroxyl radical ($^{\bullet}OH$) and related to a Fenton reaction process.[13,14] According to these authors, the two-electron oxidation expected for a peroxidase catalytic reaction does not occur on most of the "peroxidase-like nanozyme" reactions involving transition-metal oxide nanoparticles like Fe_3O_4. Instead, the oxidation observed in the presence of these nanomaterials is the result of the strong oxidation potential of hydroxyl radical formed by Fenton-type reactions driven by the Fe or other 3d transition metals.[15] Although this reaction is still been investigated a century after Fenton's first observation,[16] some of the basic, undisputed facts of the Fe^{2+}/H_2O_2 system (i.e., Fenton reaction) can be summarized as follows: (a) when Fe^{2+} ions are in excess over H_2O_2, quantitative oxidation of Fe^{2+} by H_2O_2 occurs; (b) in the opposite situation, when the peroxide is in excess over Fe^{2+}, a catalytic decomposition of the H_2O_2 takes place through $2\,H_2O_2 \rightarrow 2\,H_2O + O_2$ concurrently with the iron oxidation; (c) Fenton's oxidation process involves the formation of hydroxyl from hydrogen peroxide with a catalytic redox cycling metal.[17,18] This controversy is worth to be investigated further since it goes beyond the simple adequacy of the term "nanozyme" to the fundamental nature of the mechanisms involved, which has to be better understood if the production of reactive oxygen species (ROS) and oxidative stress in cells by nanozymes need to be mastered.

As the biologically based concept of nanozyme emerged and consolidated, it was natural to apply similar ideas to biomedical protocols and technologies. Indeed, we have witnessed a remarkable progress of biomedical technologies around nanozyme-based devices for sensing, imaging, waste scavengers, and therapeutics.[19] These new technologies are based not only on nanozyme's improved performance when compared to the natural counterparts as mentioned above but also on the evident possibility of designing their catalytic activity based on materials science knowledge.[20,21] Of course, the middle way to use engineered inorganic-biological interfaces is a reasonable strategy to improve the performance of enzymatic applications in biology, especially enzyme-based sensing devices. For instance, the use of the DNA–nanozyme interface has been reported to offer rapid and label-free colorimetric detection of *Streptococcus mutans* on dental pieces.[22] However, even non-functionalized nanozymes have been reported to have regulating properties on the cellular metabolism, notably the case of adenosine 5′-monophosphate-activated protein kinase (AMPK) that regulates cellular energy homeostasis, mostly by activating glucose uptake and oxidation when cellular energy is low. Using magnetite (Fe_3O_4) nanozymes, Zhou *et al.* have been able to control the AMPK regulating functions as an energy sensor *via* their peroxidase-like activity in the acidic lysosomal compartment.[23]

Nanozymes combining the catalytic ability with the physical properties of solid-state matter for smart response to remote stimuli (e.g., magnetic, optical, or electronic) could constitute a breakthrough for technologies such as pollutant elimination, groundwater remediation systems, nanomedicine, and biomedical devices.[24,25] Currently, the list of nanomaterials being explored as sources of catalytic mechanisms is large and diversified. The biocatalytic performance of nanozymes is currently being tested for antitumor therapeutics[26] and for other different oxidative stress related diseases, as in the case of the catalase-like activity reported in cerium oxide nanozymes against the excess of reactive oxygen species (ROS) for lowering the oxidative stress.[27]

While the general thermodynamics and kinetics involved in catalytic reactions are well understood, the microscopic mechanisms regarding nanozyme's topological and binding influence on reactivity are still being explored.[28–30] For instance, in a recent work, a Fenton-like reaction occurring at Co atoms on N-doped graphene nanoparticles was successfully modeled, using density functional theory (DFT) calculations and demonstrating that the high efficiency of CoN_4 sites was due to optimal binding energies to produce singlet oxygen activation while pyrrolic N-sites participate in the adsorption of organic molecules.[31] This type of theoretical approach seems to be the right strategy for getting a deeper understanding on the reactions involved, but it cannot be exploited adequately as long as precise data on the structural properties of the actual catalysts are scarce.

From the theoretical side, only a small number of catalytic reactions triggered by nanozymes have been fully characterized from *ab initio* quantum chemistry methods regarding the atomic mechanisms behind their catalytic performance.[32,33] The lack of experimental data of atomic-level structural mapping and magnetic states is an additional difficulty for computational models to include realistic environments. Indeed, the current challenges faced by many technological applications of nanomaterials related to their enzyme-like behavior under realistic environmental conditions are due to this lack of crosstalk between experimental and theoretical approaches. On the other side, a precise and reliable detection of free radicals produced in biological systems requires improving sensitivity of the current techniques in biochemistry, medicine, and toxicology.[34] Indeed, direct quantification of individual free radicals (especially ROS from Fenton chemistry) in cells and tissues is not currently available due to selectivity limitations and/or experimental artifacts of biochemical techniques.

Since advanced nanotechnology tools are behind the assembly of nanozymes (either by physical or chemical synthesis methods), the spectrum of composition and functions potentially attainable is almost limitless. This potentiality is reflected in the huge diversity of materials and structures already reported. Some of the most common of these compositions and the corresponding functions assigned in the literature are summarized in Table I, also indicating their active sites.

Some of the nanozymes in Table I were designed for remote activation by their intrinsic properties (e.g., optical, magnetic) and

TABLE I. Most common nanozyme activities found in the literature.

Enzymatic activity[a]	Material	Active centers	Reference
PrOx, SOx, Ox, Cat	Pt	Pt	35 and 36
SOD, Cat	Pt@PCN-Mn	Pt	37
PrOx, SOx, Ox, Cat	Pd	Pd	38 and 39
SOx, GOx, Lac, Ox, Cat	Au	Au	35 and 40
PrOx, SOD, Ox, Cat	Ag	Ag	35
PrOx, Ox, Cat	Fe_3O_4	Fe^{III}, Fe^{II}	41
PrOx, Ox, Cat	$NiFe_2O_4$	Fe^{III}	41
PrOx, Ox, Cat	MoS_2@$MgFe_2O_4$	N.A.	42
PrOx, Ox, Cat	$CuFe_2O_4$	N.A.	43
PrOx, Ox, Cat	$CoFe_2O_4$	Fe^{II}, Co^{II}	44 and 45
PrOx, SOD, GSHPx,	Mn_3O_4	Mn^{II}, Mn^{III}	46
PrOx, SOD, GSHOx, Cat	MnO_2	Mn^{IV}	47
SOD, Ox, Cat, PhEs, Nuc	CeO_2	Ce^{IV}	48
SOD, Ox, Cat	C (porous carbon)		42
Ox, Cat	C (diamond)		49
PrOx, GSHPx	V_2O_5	V^{IV}-V^{V}	50 and 51
GSHOx	$C_6Cu_4FeN_6$	Cu^{I}-Cu^{II}	52
Ox	?-MnOOH	Mn^{III}	53
PrOx	$MoSe_2$	Mo^{IV}	54

[a]PrOx, peroxidase; SOx, superoxidase; Ox, oxidase; cat, catalase; GOx, glucose oxidase; Lac, laccase; GSHOx, gultathione oxidase; GSHPx, glutathione peroxidase; PhEs, phosphoestearase, Nuc, nuclease; NOx, NADPH oxidase.

applied to catalytic reaction and subsequent recovery (and reuse), as well as to produce synergistic effects during the catalytic processes involved.[55,56] The case of iron oxide based nanozymes will be treated with some detail since this material is perhaps the most widely used in biomedical applications, and therefore their toxicity and catalytic-like behavior are of paramount relevance to establish any safety standard for their clinical uses.

In Secs. II–VII, we will discuss some of these intrinsic and extrinsic challenges to attain nanozyme efficiency and specificity comparable to biological enzymes. Despite those potential difficulties, the promising side of nanozymes is related to the ability to engineer nanomaterials to produce nanomaterials with atom-by-atom control (see, for example, Sec. IV), which can perform sequential multi-enzymatic activities. So far, most of these goals remain unachieved, despite the enormous amount of nanomaterials that have been studied.

II. NANOZYMES VS ENZYMES: THE ULTIMATE GOAL

Because nanozymes catalyze reactions that may be either beneficial or deleterious for living cells, the desired final application will determine how nanomaterials are to be designed and synthesized to achieve control of a given cell metabolic pathway. For instance, any nanomaterial would be required to suppress any intrinsic catalytic activity that could interfere in molecular or cell labeling applications,[8] while oncology therapies that rely on the generation of oxidative stress at the tumor microenvironment (TME) would require to maximize the catalytic activity to produce this oxidative stress.[57] Irrespective of the specificities of the application for a given nanozyme, what is required for its design is the knowledge of the nature of the nanomaterial at the atomic level and its correlation with the mechanisms behind their catalytic activity. A good example of this need is the recent report on the hydrolase-related nanozyme containing Zn^{2+} centers at the surface,[58] where a large increase in the cleavage efficiency of an RNA substrate was obtained by decreasing the polarity of the active site, explained by the multivalence and cooperative effect between the metal ions in this structure.[58,59] This nanozyme is the synthetic counterpart of the phosphodiesterase (PDE), a zinc-dependent hydrolase that catalyzes the cell hydrolysis of phosphodiester bonds, and therefore a complete explanation of the enzymatic mechanism will require theoretical models to assess the role of Zn^{2+} centers, the local atomic structure, and reactivity parameters.

Controlling the formation of the ROS requires a precise characterization of their surface chemistry, surface/volume ratio, the physical parameters of the environment, and precise free radical's measurement techniques. The next step in nanozyme design for biomedical purposes will require a breakthrough in the understanding of the connections between the atomic structure of nanozymes and the mechanisms leading to catalytic selectivity and/or efficiency, including Fenton-based reactions, lipid peroxidation, membrane interactions, and free radical generation. This multidisciplinary approach would only be possible only by assembling data and tools from physics, biochemistry, enzymology, toxicology, and computational modeling in quantum chemistry.

A. Why are nanozymes related to ROS?

Reactive oxygen species (ROS) is an ambiguous classification that refer to those species derived from O_2 that are more reactive than O_2. From a chemical perspective, ROS are free radicals, defined as any reactive molecular species having one or more unpaired electrons and a minimum chemical stability to exist independently.[60] All oxygen radicals happen to classify as ROS, for instance, the hydroxyl radical $^{\bullet}OH$ and superoxide anion $^{\bullet}O_2^-$ are more reactive than O_2 and thus are ROS. However, there are also oxygen derivatives having a non-radical nature, and there is no a simple way to relate the free radical character of a given oxygen species to its expected reactivity under different conditions.[61] Note also that the unpaired electron in free radicals makes them paramagnetic species.

What is the relationship between nanozymes with ROS? A concise answer is that nanozymes are intimately related to ROS because of the need for oxygen to preserve life on Earth. ROS appeared on Earth together with the first atmospheric O_2 molecules, and except for some anaerobic and aerotolerant species, all organisms require O_2 for efficient production of energy. This energy production is achieved using electron transport chains that ultimately donate electrons to O_2 (mitochondria in eukaryotic cells or cell membranes in many bacteria).[62] However, the necessity of

O_2 to maintain aerobic life also comes with a major backside, which is that oxygen gas is toxic and mutagenic. Aerobes survived only because they evolved antioxidant defenses from their anaerobic ancestors that first appeared on Earth under an atmosphere containing much N_2 and CO_2, but very little O_2. Anaerobes still exist today, but usually their growth is inhibited or even killed by exposure to the present atmospheric levels of O_2 (i.e., 20.95% mole fraction). When the O_2 content of the atmosphere rose (an event known as the Great Oxidation Event), many species must have died out, but the survivor present-day anaerobes are mostly the descendants of organisms that followed the evolutionary path of "adapting" to rising atmospheric O_2 levels. For an excellent biological and historical review of the rise of complex life, the reader is referred to the work of Taverne *et al.*[63] The survival strategy of these organisms was to develop antioxidant defenses (evolving new ones as well as realigning ancient molecules to new functions) to protect against O_2 toxicity. The first modern hypotheses about oxygen toxicity suggested that O_2 directly inhibited essential enzymes, but it was later recognized that the inactivation rates by O_2 are too slow to explain O_2 toxicity. A seminal work from Gerschman *et al.* in 1954 drew a parallel between the effects of O_2 and ionizing radiation, proposing that the damaging effects of O_2 were due to oxygen radicals.[64] Today, there is an established consensus that ROS are also important signals that regulate numerous processes during cell life, and the idea that cell management of ROS as regulators of cellular signaling pathways should actually be considered a key evolutionary step has been suggested.[63] Indeed, ROS are essential molecules in neuronal development and nervous system function,[65] challenging previous assumptions that ROS were just by-products of the mitochondrial respiratory chain.[66] It is because our evolutionary history that enzymes, and thus any potential nanozyme's application in biology, are bounded to ROS.

The relation between nanozymes and ROS further extends to environmental applications. Natural and urban water systems contain a diversity of ROS produced from natural organic matter and man-produced organic pollutants, including singlet oxygen ($^1O_2$), hydroxyl radicals ($^{\bullet}OH$), superoxide anions ($^{\bullet}O_2^-$), and H_2O_2 induced photochemically (i.e., sunlight). The need of O_2 in aerobes requires a simultaneous ability to manage the high toxicity of oxygen to survive, developing biochemical antioxidant defenses.[67] At physiologically "normal" O_2 levels, all aerobes are exposed to oxidative damage, mainly from the superoxide radical ($^{\bullet}O_2^-$).[68,69] From the perspective of human health, the general consensus is that increased levels of free radicals and the consequent oxidative damage show correlation with aging and some neurodegenerative diseases.[67,70] In this context, ROS have long been studied as toxic agents with a role in nervous system aging and deterioration through neurite degeneration before cell death.[71]

III. THE CATALYSIS VIEWPOINT

The recognition on enzymes as biological catalysts date back to more than a century ago when the amylase's hydrolytic activity on starch was proposed.[72] Subsequent research on these types of mechanisms opened the whole field of enzymology to understand the vast catalytic reaction pool of cell biochemistry and the exquisite specificity that balance most life reactions. However, major obstacles to develop a wide-ranging picture for the catalytic properties of enzymes are due not only to enzyme diversification along different evolutionary paths but also to the highly non-linear and feedbacked nature of the reactions involved that make useless the basic approach involving reduction and partitioning of catalytic contributions into independent and energetically additive components. These issues are beyond the scope of this work, and for a more historical view of these difficulties, the reader is referred to the thoughtful work by Heckmann and Paradisi.[73]

The significance of enzymes as catalysts relies on the fact that they speed up reactions that are thermodynamically favorable but have too-slow kinetics compared to the time scale compatible with life. Enzymes' way to enhance the velocity of a reaction is by lowering the energetic barrier through the alignment of reactive groups, the formation of transient unstable charges, bonding reorganizations, and other transformations that are crucial but very unlikely to take place freely in the cellular environment. In other words, enzymes provide a propitious ambient for the reaction to take course, known as the active site (see Sec. III D). Active site has a critical role in enzyme activity and catalytic mechanisms since its functional groups generate the conditions for an alternative route for chemical reaction to occur in a way that lowers the activation energy.[74] In enzymes, the active site represents a confined space or pocket within the enzyme's structure where the initial bonding of the specific substrate (bonding site) and the catalyzed reaction (catalytic site) takes place. This particular arrangement that combines specific amino acids, topology and conformation, and its participation is a distinguishing feature of an enzyme-catalyzed reaction.

Similarly, nanozymes offer a site that promotes a similar scenario during catalysis. Although not as conventionally described as in enzymatic active sites, certain atoms and arrangements of atoms within the structure of the nanozyme are responsible for the specific and proper catalytic activity. Despite the advantages of nanozymes over natural enzymes mentioned above, a clear weakness of the former is their poor catalytic performance, which is still lower than natural enzymes in most cases. Perhaps more important is the fact that nanozymes' specificity could be fundamentally limited because nanomaterials lack the flexibility at the bonding site that is provided by the organic-based local environment at the active site in natural enzymes, which is responsible for restricting non-specific substrates to enter the enzyme pocket. This flexibility of some natural enzymes also allows changing their conformation during reaction, as a way to function through different mechanisms by which its function is regulated to improve activity and specificity. Figure 1(a) shows a scheme of the different roles for these elements, including substrate binding, involved in the regulation of enzymes activity. In Fig. 1(b), the effect on enzyme conformation is exemplified by the hexokinase 6 changes after ADP-PO_4-Mg^{2+} substrate binding. The comparative situation for nanozymes [magnetite in Fig. 1(c)] shows that reactions at the particle surface involve eventual changes of the chemical structure but not its conformation/topology, activity, and/or specificity. It is important to note that these regulatory mechanisms are critical not only for catalysis efficiency but also for the regulation of their biological activity because they must work within an intracellular medium with large amounts of different substrates and in a time-coordinated way (even in synchrony) with other cellular events.

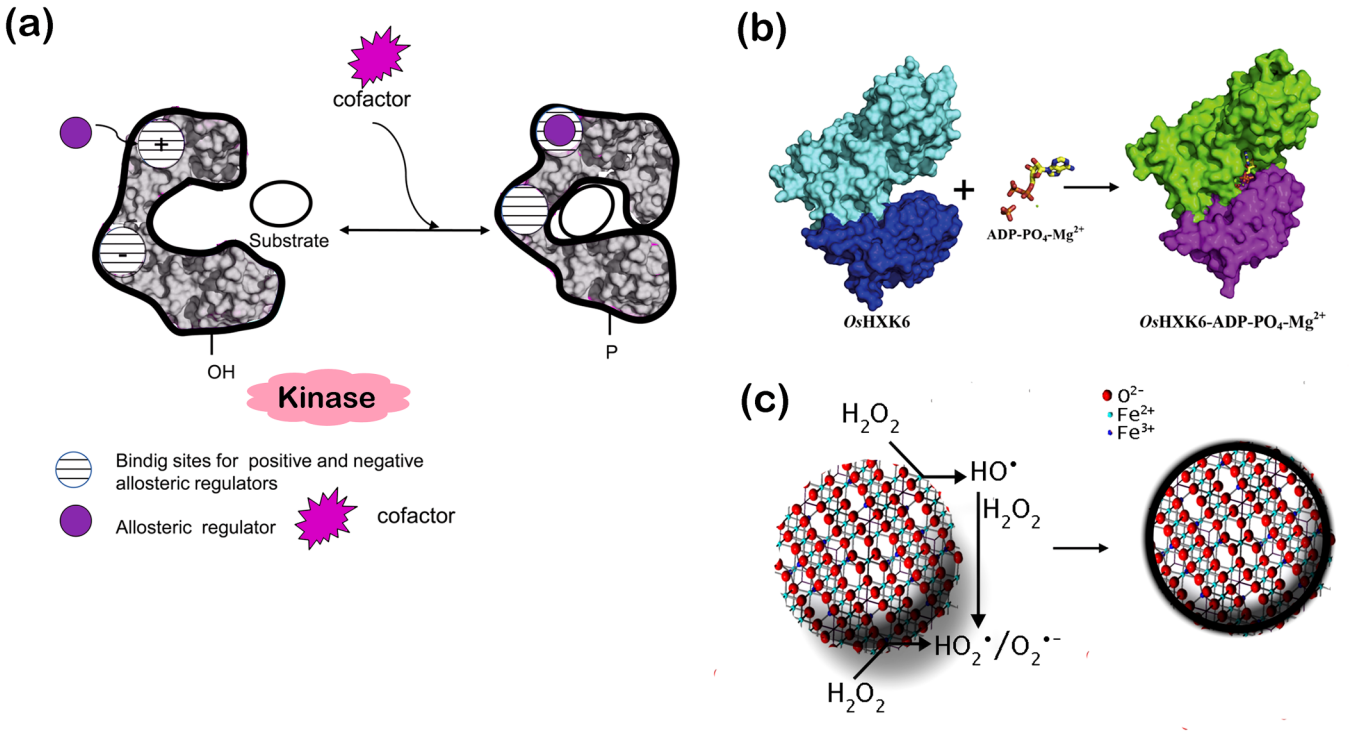

FIG. 1. (a) Enzyme regulation and conformational changes in the presence of allosteric regulators, substrates, cofactors, and post-translational modifications. (b) Crystallographic structure based 3D model of hexoquinase 6 before and after substrate binding. (c) Nanozyme, iron oxide nanoparticles, and surface modification during H_2O_2 oxidation.

The catalytic activity of nanozymes depends directly to the coordination of the active ion at the surface of the material, especially for metal-based nanozymes.[75] The ability to buildup materials with fine control on the structure and composition of the surface at the atomic level is at the root of future designs of functional nanozymes, and this task will thus require a complete atomic characterization and modeling of the active sites using advanced characterization techniques at large scientific facilities,[76–78] with further correlation of these data to the catalytic activity under different conditions. This level of understanding of the correlation between the structure and composition at the atomic level and the ability to design nanozymes with optimal catalytic activity are far from complete, but it could be argued that the present stage of nanozyme development has already produced enlightening and promising results, shading light on the key problems to be addressed.

In this regard, three main perspectives can be mentioned according to nanozymes' application: achieving specificity, regulation of their activity, and enhancing catalytic activity. Although, specificity and regulation are not requirements for some applications, i.e., chemical reactions or degradation of water contaminants, it is mandatory for biological applications in diagnostics or treatments based on nanozymes' activity. In order to emphasize each problem, we are going to discuss the actual approaches to overcome these issues separately in Secs. III A–III D.

A. The kinetics of nanozymes

One of the simplest and best-known methods to explain enzyme's kinetics on different substrates is the Michaelis–Menten model.[79] It asserts that during an enzymatic reaction, a substrate *S* is transformed into a product *P* by a given enzyme *E*, through the formation of an intermediate complex ES in the sequence

$$E + S \rightleftharpoons ES \rightleftharpoons E + P.$$

The rate of this reaction depends on the instant concentration of substrate [S], a fact that complicates the measurement of any *in vitro* catalytic reaction while a given substrate is being converted to product. For this reason, a basic approach in kinetics experiments is to measure the initial velocity V_0 of the reaction since usually, under intracellular conditions, the enzyme's concentration is many orders of magnitude smaller than the concentration of substrate ($[E] \ll [S]$). In this situation, at the initial times of the reaction, the changes in [S] should be small enough to be disregarded and considered constant. The discussion of even the basic concepts of catalysis kinetics is beyond the scope of this review, and the reader is referred to classical literature studies for these topics.[74,80,81]

Enzymatic kinetics often helps elucidate the number of steps by which enzymes convert the substrates into products and, hence,

the reaction order. It also gives valuable information about enzyme regulation by different compounds that affect its activity, such as activators or inhibitors and whether they are competitive or non-competitive. It has also been used to elucidate the active site amino acid composition through site-directed mutagenic studies and to characterize nanozymes' activity by using the same substrates of the natural enzymes. In fact, although nanozymes behave different than natural enzymes, this approach has also been proposed as a standardized method to compare the intrinsic peroxidase-like activity of different nanoparticles.[73] The "learning-from-nature" approach, i.e., to mimic enzyme active sites for a nanozyme design, is a valuable tool for manufacturing and activity optimization, and the final goal is to develop structures that can fully reproduce the natural active sites in enzymes.[82] Identifying the catalytic site in natural enzymes has been one of the goals of classical enzymology, which allowed us to understand the reaction mechanism and the possibility of catalysis improvement. Identifying the active site in nanozymes is not trivial, and for many materials/enzymes, it is not well established. The development of methods to test reaction mechanism hypotheses along with the design and engineering of desired activities should contribute to solve some of these issues. Interestingly, for some well-established activities, active sites have been recognized and proven, and reaction mechanisms have been proposed and validated. One remarkable thing to mention is that in many cases, the same enzymatic activity can be mimicked by different nanomaterials, a potential advantage for different reaction conditions. Interestingly, the same behavior can be observed for enzymes where members from different families with quite different structures can catalyze the same reaction.

Among the different concepts to improve the kinetic performance of nanozymes, the single-atom nanozyme is so far the most promising. Although these entities have the same origin and properties than nanozymes, they are found in the literature also under the names of single-atom catalysts (SAC) or single-atom nanozymes (SAzymes). In Secs. III B–III D, we will use these names following the nomenclature of those works under review. Different types of SACs have been developed since the 2000s from the classical field of gas–solid heterogeneous catalysis,[83,84] but only since 2010–2012, the enzymatic-like properties of SACs have been considered from a biomedical perspective and it is this novel approach that we will consider below.[85–87] The basic idea of SACs is to produce a more complex architecture of the nanomaterials consisting of atomically dispersed sites over some (inert or synergic) surface. The isolated single atoms, stabilized by the support, provide the active sites (usually metal species) for heterogeneous catalysis. The strong metal–support interactions in SACs allows a low coordination environment and the charge-transfer effect that would explain the enhanced intrinsic activity of the active sites.[29]

A related type of SAC based on iron–nitrogen graphene oxide embedded (Fe–N–rGO) that resembles the heme-cofactor present in natural horseradish peroxidase (HRP) has been recently synthesized by Kim *et al.*[88] By doing this, the authors were looking not only for a higher activity but also for substrate and reaction specificity/selectivity. They hypothesized that the Fe–N–rGO structure would have intrinsic peroxidase activity and selectivity by mimicking the active site of natural peroxidase, which is known to be responsible for enzyme properties (see the scheme in Fig. 2). In this work, the similarity among the natural enzyme active site and the Fe–N–rGO structure was exhibited, and specific peroxidase activity was described and characterized relative to iron NP, Pt (111), and HRP (the natural enzyme). The authors found that Fe–N–rGO was specific in its peroxidase activity and showed very high activity, while other nanozymes also show oxidase, catalase, and superoxide dismutase (SOD) activity. Although they did not validate a reaction mechanism, they clearly showed that both Fe and N were necessary for the achieved activity and that the configuration/conformation of the atoms arrangement (active site) was very similar to that of the natural HRP active site. In addition, five steps and their free energies were tested by DFT for Fe–N–rGO and other catalysts. The DFT calculations and experimental results confirmed that the material had high activity and specificity for the peroxidase-like reaction [Fig. 2(b)]. These types of studies should help not only to understand the reaction mechanisms and performance of already established nanozymes but also to make an impact in nanomaterials with enzyme-like activity design and optimization, for old and new substrates. In addition to catalysis improvement, SAC studies can contribute to the development of the nanozyme field since their simpler structure (as compared to natural enzymes) facilitates the identification of active sites and, thus, using theoretical models, the possibility to predict and corroborate the different reaction mechanisms. Although these tools and strategies for understanding nanozymes resemble those approaches used in enzymology along several decades, it is important to note that the inorganic chemistry involved in synthetic nanozymes will allow the use of novel and well-established experimental and theoretical tools from condensed matter sciences.

B. Achieving specificity

As pointed out previously, the very first step for enzymes to lower activation energy is to bind the substrates in the binding residues of the active site through multiple weak interactions. Then, as enzymes' active sites are complementary in structure to the transition state of the reaction, the reaction takes place in the catalytic part of the active site. However, this is not the case for most nanozymes that possess the catalytic activity but lack the binding functional groups that give the specificity and efficiency to the reaction. In this regard, numerous efforts have been made to overcome this issue and all of them are focused on emulating the active site. Common strategies concerning the improvement of the activity of the nanozyme are focused on the control of the morphology, crystallinity, size, exposed facets, composition, and doping with heteroatoms or the use of hybrid materials with interfacial effects.[89] The presence of specific ligands could also regulate the activity of nanozymes.[90] Concerning the substrate specificity of the enzyme-like activity of nanozyme, there are several research lines based on the strategy of conjugation that endows the presence of substrate-binding sites with superficial molecules,[58] imprinted polymers,[91,92] or biomolecules such as aptamers.[29] Another possible strategy to improve both the activity and substrate specificity is to used nanozyme assemblies or combined structures containing nanozymes and natural enzymes.[93,94]

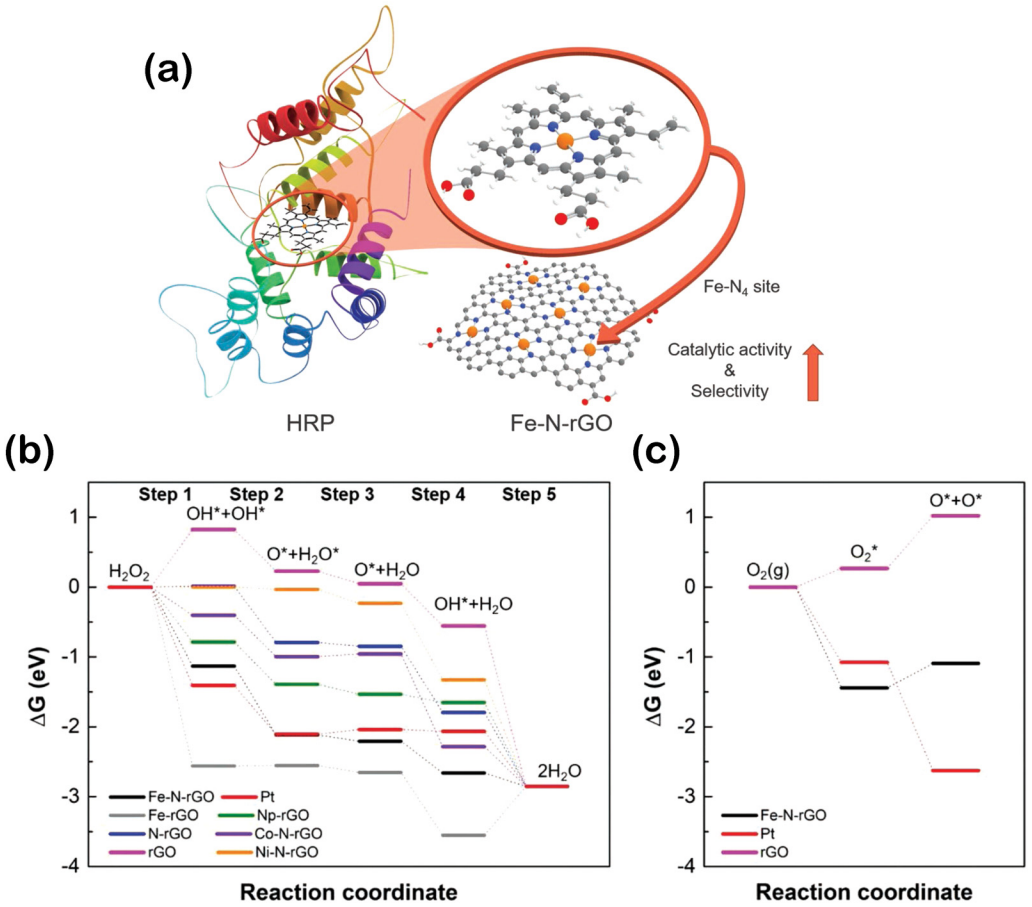

FIG. 2. (a) Heme-cofactor-resembling Fe–N single site embedded graphene as nanozymes to selectively detect H_2O_2 with high sensitivity. (b) Energy profile for peroxidase-like reaction on the six types of graphene structures (Fe–N–rGO, Fe–rGO, N–rGO, rGO, Ni–N–rGO, and Co–N–rGO) and Pt and (c) oxidase-like reaction on rGO, Fe–N–rGO, and Pt. Reproduced with permission from Kim *et al.*, Adv. Funct. Mater. **30**(1), 1905410 (2020). Copyright 2021 John Wiley and Sons.

C. Regulating nanozyme activity: The case of the peroxidases

Enzymatic activity can be regulated in many ways that usually involve enzyme protein configuration changes. This property has been difficult to mimic with inorganic matter and has, therefore, been a major concern for biological applications of nanozymes *in vivo*, although there is plenty to learn from nature to solve this problem. The example of peroxidases is in this sense only illustrative. Peroxidases are widely represented across all kingdoms, and their active site and catalytic mechanism have been extensively studied. These enzymes are hemoproteins that react with hydrogen peroxide to form highly reactive intermediates, which oxidize peroxidase substrates. Human peroxidases can be divided into true- or pseudo-peroxidases and according to whether they can exert peroxidase or peroxidase-like activity, respectively, as depicted in Fig. 3. There are many true peroxidases that differ in their active site and, hence, in their substrate specificity. As a common feature of true

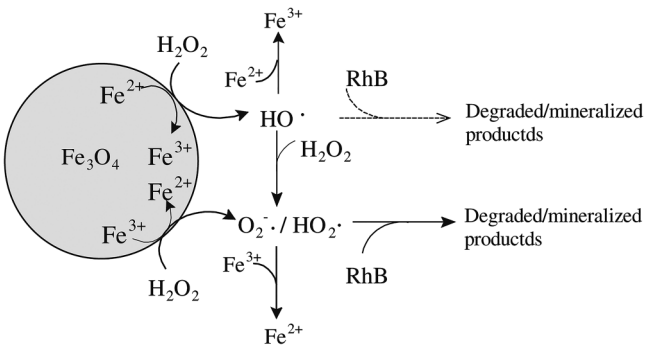

FIG. 3. Mechanisms for the activation of H_2O_2 on the peroxidase-like Fe_3O_4 MNPs catalyst in the degradation of organic pollutants. Reproduced with permission from Wang *et al.*, Ultrason. Sonochem. **17**(3), 526–533 (2010). Copyright 2010 Elsevier.

peroxidases, they do not have oxidizable amino acids in their active site, and they combine a peroxidase cycle, in which free radicals are generated, with a halogenation cycle, in which (pseudo)hypohalous acids are obtained.[95]

On the other hand, pseudo-peroxidases are hemoproteins that are not meant to react with hydrogen peroxide, like hemoglobin. They possess oxidizable amino acids in close proximity to the heme group and under certain conditions acquire peroxidase-like activity through active heme compounds formation and protein-based radicals intermediates, such as tyrosine and tryptophane. In a similar (to some extent) way than for classical nanozymes, once the reaction products are obtained, they lose their function. In pseudo-peroxidases, this is due to protein cross-linking and aggregation; in the case of Fe_3O_4 nanozymes, this is due to changes in iron oxidation state.[9] In this sense, SACs' activity is more related to true peroxidases while conventional nanozymes' activity is more related to pseudo-peroxidases due to the fact that after catalysis, enzymes are recovered unchanged while nanozymes are reduced or oxidized during the reaction.

An analogy can be made with nanoparticles that exhibit peroxidase-like activities. Iron oxide nanoparticles' peroxidase activity was reported first by Gao *et al.*,[8] who described how the iron oxides could catalyze the oxidation of different substrates under different conditions of pH and temperature. Their experimental data suggested that Fe_3O_4 nanoparticle mechanism of action begins when an H_2O_2 molecule undergoes homolytic cleavage, with the O—O bond cleaving to form two hydroxyl radicals, which would then capture a proton (H^+) from a hydrogen donor. Few years later to its discovery, Wang *et al.*[96] described a precise mechanism that included the confirmation of surface reaction. In this work, the degradation of organic pollutant by $H_2O_2^-$•Fe_3O_4 peroxidase mimetic activity was studied. The authors confirmed that $^{\bullet}OH$ was critical for reaction initiation, but they found that $^{\bullet}O_2^-/^{\bullet}HO_2$ were the main ROS involved/contributing to organic compound degradation (see Fig. 3).

According to what was previously stated, the mechanism of action differs among peroxidases, pseudo-peroxidases, and nanozymes, and regulation approaches are quite different as well. Myeloperoxidase (MPO), is a perfect example of a true-peroxidase capable of generating significant amounts of HOCl in acidic inflammatory environments, where H_2O_2 steady-state concentrations are also increased.[97] MPO activity is carefully regulated to avoid healthy tissue damage by keeping away larger molecules to enter the active site by its union to inhibitory proteins, such as ceruloplasmin, and by neutral pH.[98] Likewise, efforts to regulate nanozymes activity for *in vivo* applications involve pH-sensitive control of nanoparticle release in inflammatory tissue,[99] redox-responsive systems,[100] temperature[101] and even a combination of photothermal therapy with enzymes, like glucose oxidase (GOD), that convert glucose into glucuronic acid with H_2O_2 release for Fe_3O_4 nanoparticles to catalyze Fenton -based reactions.[102,103]

The case of the peroxidase activity is a good example of the way to figure out which strategy to follow and what can be achieved by combining the knowledge of enzymes and the advances in science material toward to better mimic enzyme activity. This is not only due to the nature of the peroxidase active site, a metalloprotein, but also due to the fact that we have extensive knowledge of the heme prosthetic group. In addition, ion oxides' peroxidase-like activity was one of first nanomaterials to be discovered and consequently extensively studied. Improving the flexibility and specificity of nanozymes will, therefore, require combining the knowledge already gained from enzymology and translate those functionalities to nanozymes, being either through similar mechanisms or radically different ones.

A broader approach to improve catalytic activity in nanozymes has been recently reported, based on the use of hybrid systems combining biomolecules–nanoparticles or metalorganic systems.[104,105] This constitutes an interesting tactic to stimulate the bio-electro-catalyzed oxidation of glucose by the electrical contact of an integrated enzyme electrode that stimulates the bio-electro-catalyzed oxidation of glucose. A recent work by Katz *et al.*[106] reported a related scheme through the use of an apo-flavoenzyme with a relay-FAD-cofactor dyad, electrically contacting them to obtain a hybrid (named electroenzyme), while the engineering of the apo-glucose oxidase (apo-Gox) was achieved using a ferrocene-tethered FAD-cofactor. The strategy of covalent linkage of aptamer binding sites to nanozymes has the advantage of versatility and better catalytic activity compared to values reported so far for "pure inorganic" nanozymes. Current efforts on these hybrid systems are being focused on assembling reaction substrates at the catalytic nanozyme core to emulate the binding and catalytic active site functions (as discussed in Sec. III D) of native enzymes.[107]

D. The active site

Although many of the chemical reactions involved in living organisms are thermodynamically favorable, they would take time on the scale of years to occur. Thus, catalysis in biology is essential to speed up those reactions so they can occur in a time scale compatible with life. Catalysts enhance the velocity of a given reaction without altering its chemical equilibrium, by lowering the energy barrier through the alignment of reactive groups, by the formation of transient unstable charges, by bonding reorganizations, etc. The active site provides the favorable atomic environment to make this possible. In biological enzymes, the active site represents a confined space or pocket within the enzyme's structure where the catalyzed reaction takes place. This precise arrangement that combines specific amino acids, topology, and conformation, is the fingerprint of an enzyme-catalyzed reaction. The extreme efficiency of natural enzymes is the result of millennia of natural evolution, and therefore they have been the inspiring background to emulate some of their characteristics when nanozymes are designed and engineered, an activity that has been recognized and termed "learning from nature." In classical enzymology, the advancements on the identification of the subtle relationships between active sites and reaction mechanisms were boosted by the incredibly rapid increase of structural data, freely available in libraries of enzyme superfamilies (as the Protein Data Bank, PDB)[108] with thousands of detailed structural data files. As a consequence, the current state in the field offers many examples of complete reaction explanations of atomistic mechanisms in exquisite detail combining enzyme structure characterization, active site topology, and numerical modeling from first principles.[84,109,110] It can then be expected that advancements on the specifics of nanozyme's reaction mechanisms will require an

analogous strategy for gathering and sharing the relevant data of crystal structure, chemical composition, electronic configuration, etc.

The dynamic nature of the protein cage surrounding most active sites in biological enzymes has also been recognized, posing further challenges for nanozyme's mimicking of their natural counterparts.[111,112] There is consensus about the subtle relationship between the function of active sites and the surrounding protein dynamics for a given enzymatic function. It has been proposed that a previous adaptation of the enzyme's active site environment to specific substrate topologies allows the selection of those substrate subsets that approach the configuration of the relevant transition state.[113] This would eliminate the slow components and thus would speed up the reaction. It is yet to be proven whether similar high enzymatic rates can be achieved in nanozymes without the need of the plasticity provided by the protein cage.

IV. STRUCTURAL ATOMIC UNDERSTANDING OF NANOZYMES

Nanozyme characterization is a crucial aspect for the improvement of these materials. The lack of detailed structural knowledge, especially at the atomic scale, is currently a limiting factor on nanozymes' development because of the need of these experimental data at the atomistic level to provide a realistic input for theoretical calculations. Among the general properties to be characterized, the most important ones include the size and morphology of the particles, structural aspects such as crystallographic data and location of active sites, chemical composition, or specific surface area, among others. This section discusses some of the most used characterization techniques with special emphasis on electron microscopy and how this technique can reveal features not accessible by other methods.

Dynamic light scattering (DLS) is a relatively common and fast method to characterize the hydrodynamic size of nanozymes.[114,115] DLS can be used to study the surface modification of nanozymes by comparing the data obtained by this technique vs the data obtained from transmission electron microscopy (TEM). The latter technique usually yields smaller values than DLS on the same materials, and from this difference, basic information on the species bonded to the surface can be inferred. More evidence on these bonded species can be obtained from the ζ-potential of the nanozyme,[116] an indicator of the nanozyme's surface charge and a key factor for the catalytic specificity for a given substrate.[117]

To determine functional groups bound to the nanozyme's surface, as well as surrounding molecules, Fourier transform infrared (FT-IR) spectroscopy is often used. Its high spectra resolution and high sensitivity make this technique a common method to corroborate the formation of nanozymes through surface functionalization.[118–120] FT-IR is also used as a potential tool to study the catalytic activity of nanozyme directly by changes in the nanozyme or by changes in a substrate and original reactive products through kinetic sequential measurement, allowing us to study the kinetics and order of the reactions.[121] In addition to FT-IR, Raman spectroscopy can provide information on the vibrational and electronic modes of the sample, which is particularly useful for studying materials in aqueous solutions as well as biological materials due to the weak signal of water. The main complexity of this technique is the low quantum efficiencies, and therefore the signal needs to be amplified in what it is named surface-enhanced Raman spectroscopy (SERS);[122,123] for instance, Wen *et al.*[124] were able to produce an excellent semiconducting SERS substrate, which presented high oxidase-like activity that was used to monitor the catalytic process, This work revealed a better affinity between the enzyme and the substrate, thus confirming the actual enzyme-like mechanism at the surface of the nanozymes.

When comprehensive information about the chemical structure and composition is required, XPS (x-ray photoelectron spectroscopy) is generally regarded as being the most quantitative and informative technique. XPS uses x-ray radiation in the range of 0.2–1.5 keV to produce a stimulated emission from the valence or inner electrons located at 10–200 Å (depending on the sample and instrumental conditions) from the top surface. The energy of the excited photoelectrons measured[125,126] provides local information on the chemical composition and on the oxidation state and bonding of the components, except for hydrogen and helium, of any solid surface that is vacuum stable or can be made vacuum stable by cooling. XPS has been used to reveal the structure–activity relationship of carbon nanospheres with a zinc-centered porphyrin-like structure (PMCS),[127] confirming the chemical composition of all samples indicating the presence of C, O, N, and Zn. By observing the N 1s spectra, it was possible to study the chemical bonding between the C and N; for the starting material (i.e., zinc-based zeolitic imidazolate framework, ZIF-8), a sharp peak assigned to C═N of 2-methylimidazole was observed. However, after high-temperature pyrolysis a different peak appeared at 401.2 eV, which corresponded to graphitic N in the PMCS.

Perhaps, the most extended technique for analyzing the structural properties of most materials, including nanozymes, is x-ray diffraction (XRD) in powder samples (PXRD). From PXRD, it is possible to acquire information on the crystallinity of a material to identify the crystalline phase or, in a less accurate way, obtain information on the composition and particle size.[128,129]

One of the most advanced characterization methodologies that encompass many of the structural information required is transmission electron microscopy (TEM).[130] Chemical composition, oxidation states, and even chemical bonding can be studied by spectroscopic techniques including energy dispersive x-ray spectroscopy (EDS) and electron energy loss spectroscopy (EELS). Structural information can be obtained by electron diffraction in a similar way as performed by PXRD with the advantages that small crystallites can be considered single crystals and, therefore, the volume required is of several orders of magnitude smaller than for XRD. In fact, crystals as small as 50 nm can be fully solved by electron diffraction methods.[131] Among the many advantages of TEM over other characterization methods is that it combines spectroscopic analyses with diffraction and imaging; therefore, besides solving the crystal structure with sub-angstrom resolution, it also provides particle size distribution. Conventionally, image analyses have been performed using a parallel beam in this TEM mode; however, complementary to this mode, the electron beam can be controlled to converge into a small probe that scans over the sample, a modality known as scanning transmission electron microscopy (STEM).[132] In the STEM mode, images are formed

using various detectors than can be simultaneously used; a high angle annular dark field (HAADF) detector displays an image where the contrast is dependent on the atomic number of the elements allowing us to obtain chemical information as well as structural observation at atomic level.[133] STEM has played a crucial role in nanozyme characterization as it has been used to obtain information of the particle size and morphology and also to achieve atomic information of active sites, especially in the recent subarea known as single-atom nanozymes (SAzymes). The location of the active sites and how they are anchored within the support and related to the surrounding environment are key points in nanozyme development. In the first work reporting the peroxidase-like activity exhibited by Fe_3O_4 nanoparticles,[134] also the structural and morphological characterization were performed using TEM and, since then, the use of this technique has been associated with almost every report in this field. In 2019, Wang *et al.*[135] studied the effect of Co doping Fe_3O_4 NPs in order to increase their affinity for killing renal tumor cells. The size and morphology of the *as-synthesized* nanozymes were evaluated by conventional TEM before and after Co doping [see Figs. 4(a) and 4(b), respectively] observing no significant changes between both nanozymes that, however, displayed different activations associated with the presence of Co.

Deeper structural investigations by means of high-resolution transmission electron microscopy combined with scanning electron microscopy (SEM) were applied to characterize the size, morphology, and crystalline structure of Fe_3O_4 nanocrystals. In this work, Zhu *et al.*[136] investigated how the morphology (spheres, octahedral, and triangular plates) affected the TMB (3,3′,5,5′-Tetramethylbenzidine) oxidation observing a superior affinity of the spherical NPs for TMB as a result of the highest surface area. Interestingly, triangular shaped NPs exhibited slightly higher activity in comparison with the octahedral ones. This behavior, revealed by a high-resolution TEM study, was attributed to the higher reactivity of the [220] planes with respect to the [111] ones owing to the open plane and dangling bonds [Figs. 4(c)–4(e)]. Additional contributions from HRTEM include the determination of morphology and structure of CeO_2 nanoflowers,[137] the morphology MnO_2@PtCo nanoflowers (with the composition corroborated by TEM-EDS),[31] investigation of V_2O_5 nanowires that mimic the antioxidant enzyme glutathione peroxidase

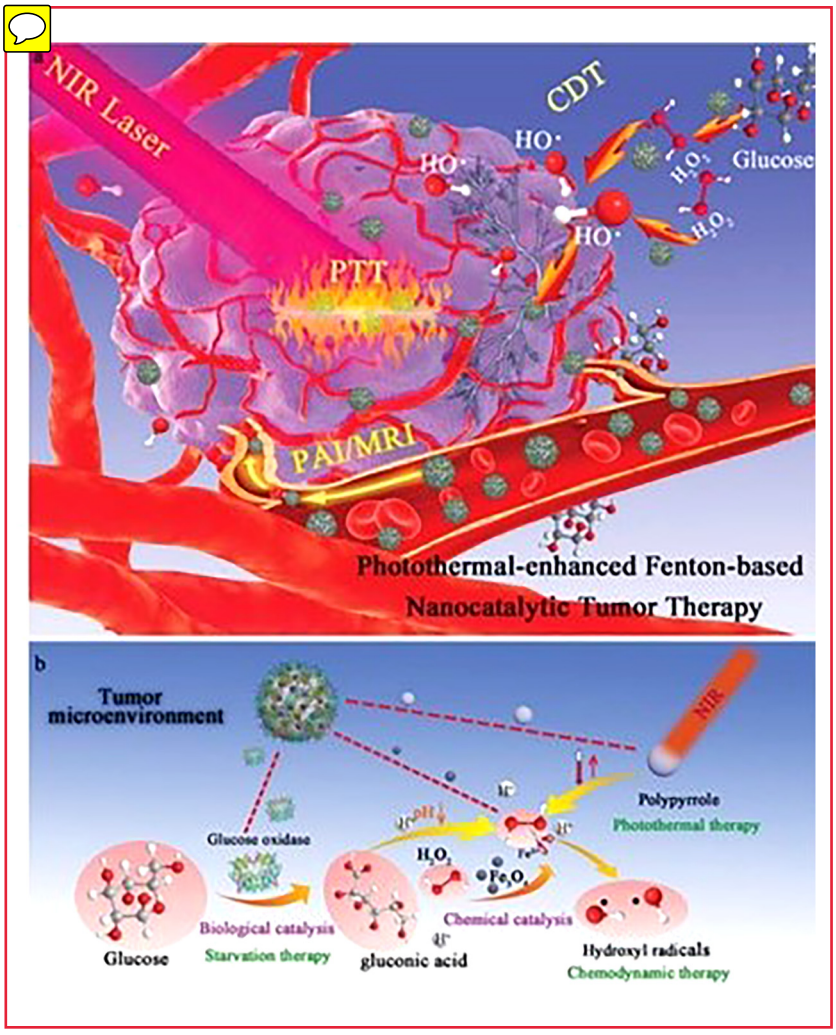

FIG. 4. (a) TEM images of the Fe_3O_4 and (b) Co@Fe_3O_4 nanozymes used for the treatment of tumor cells. Adapted from Huang *et al.*, Sci. Adv. **5**, eaav5490 (2019). Copyright 2019 Wiley-VCH. (c-1), (d-1), and (e-1) SEM data of Fe_3O_4 nanocrystals corresponding to spheres, octahedral, and triangular plates, respectively. (c-2), (d-2), and (e-2) TEM micrographs of individual particles for spheres, octahedral, and triangular plates, respectively. (c-3), (d-3), and (e-3) High-resolution data obtained for each morphology, with the d-spacing associated to different facets (inset). Figure adapted from Liu *et al.*, Chem. Eur. J. **17**, 620–625 (2011). Copyright 2011 Wiley-VCH.

by using cellular glutathione,[138] and the analysis of carbon based nanozymes.[31,139–141] Aberration-corrected STEM-HAADF is so far the only technique that allows direct observation of the single atom (metal) on a given substrate, which is critical information for any DFT model of SAzymes.[137,142]

Among the many carbon-supported SACs developed for catalysis, sensing, degradation of organics because of their good stability, surface area, and flexibility with dopants, there are some that are particularly adapted to mimic enzymatic activity. The metal coordination is usually achieved through N forming a complex of $MetalN_x$ anchored to the carbon support, which provides the ability to mimic the behavior of natural enzymes; in this sense, Ma *et al.*[143] reported on a novel SAzyme using iron atoms as active sites, in the form of FeN_4, on porous carbon materials. They were able to mimic two antioxidative enzymes of catalase (CAT) and superoxide dismutase (SOD) serving as bifunctional materials able to scavenge reactive oxygen species generated during oxidative stress in cells through the catalytic decomposition of H_2O_2 into H_2O and O_2 and O_2^- into H_2O_2 and O_2. The approach taken in that work was to encapsulate iron phthalocyanine (FePc) inside the cages of a metalorganic framework (MOF) and zeolitic imidazolate framework (ZIF-8), followed by a high-temperature pyrolysis process. After ZIF-8 decomposition, the material was characterized by TEM [Fig. 5(a)] observing that the as-synthesized material presented an average particle size of around 50 nm and somehow preserved some the morphological features of the parental material (dodecahedral shaped particles). However, the presence of Fe atoms was not evidenced by TEM and, therefore, Cs-corrected STEM-HAADF was used, observing the presence of bright spots associated to the existence of single Fe atoms (red circles) [Fig. 5(b)]. Chemical mapping was also employed to corroborate the homogeneous distribution of C, N, and Fe. Within this work, electron microscopy was employed to characterize the morphology, size, and composition of the nanozymes, evidencing as well the generation of single Fe sites; however, it did not reveal the metal–carbon coordination. To investigate the local structure at an atomic level, the authors turned to x-ray absorption near-edge structure (XANES) and extended x-ray absorption fine structure (EXAFS) measurements at Fe K-edge. Figure 5(c) depicts the XANES curves of the FeN_4 nanozyme together with the references of Fe foil, FeO, and Fe_2O_3, suggesting that the Fe valence was between +2 and +3. Least-squares EXAFS fittings [see Fig. 5(d)] gave a coordination number for Fe of about 4 with bonding lengths (between Fe and surrounding N atoms of 2.01), allowing us to conclude that the local atomistic structure of Fe was composed of Fe isolated atoms coordinated to four N, which were subsequently linked to the C structure, see the inset of Fig. 5(d).

A similar methodology for the generation of SAzymes by Huang *et al.*[135] was applied to study the oxidase catalytic reaction as a model reaction, combining experimental studies with theoretical calculations to observe the existence of single-atom active sites within carbon nanoframes. In this case, a coordinated complex formed by FeN_5 was responsible for stabilizing the reactive sites, which were responsible for the oxidase-like activity as a result of the synergistic effect and electron donation mechanism. The nanozyme was achieved by encapsulation phthalocyanine (FePc) within a MOF (Zn-MOF), which was subsequently pyrolyzed at 900 °C. TEM combined with Cs-corrected STEM-HAADF were used to study the morphology of the pyrolyzed material as well as for identifying (barely) the Fe atoms.

A more precise approach, from an electron microscopy perspective, was reported by Deng and co-workers[144] where they were able to immobilize isolated Fe atoms in a graphene matrix through the formation of FeN_4 centers used toward the oxidation of benzene to phenol at room temperature. The structural analysis was carried out by aberration-corrected TEM (ACTEM) and by Cs-corrected STEM-HAADF electron microscopy together with low-temperature scanning tunneling microscopy (STM). The typical morphology of the FeN_4/graphene nanosheets (GNs) is depicted in Fig. 6(a), obtained by ACTEM recorded at 80 kV to minimize the electron beam damage, where red arrows pointing at black dots indicate the presence of Fe atoms. A closer observation of these sites is presented in Fig. 6(b). The region framed by a dashed red circle is attributed to one of these Fe sites, while the correspondent atomic model is shown in Fig. 6(c), matching perfectly with the density functional theory (DFT)-simulated data, which were also calculated by Deng and co-workers. To further corroborate that those black dots were Fe atoms, Cs-corrected STEM-HAADF was also employed to visualize the structures, which showed the atomic size and homogeneous distribution of bright spots (Fe atoms) along the graphene matrix [Figs. 6(d) and 7(e)]. Additionally, atomic-resolution spectroscopic measurements were also carried out by means of electron energy loss spectroscopy (EELS), obtaining the signals corresponding to Fe and N, suggesting the formation of $Fe—N_x$ bonding. To gain additional structural and electronic information, low-temperature STM was performed observing a similar configuration to that reported by electron microscopy. Furthermore, the scanning tunneling spectroscopy (STS) measurements showed a sharp resonance state at −0.63 eV below the Fermi level, which would indicate that the Fe would be strongly interacting with the C matrix introducing a new electronic state near the Fermi level.

SAzymes have also been used for pollutant degradation a reaction that has been traditionally carried out by natural enzymes.[145,146] However, nanozymes when they are used as ROS generators can offer certain advantages over natural ones such as low costs, high activity, and the possibility of recyclability. He *et al.*[147] prepared Fe–N–C single-atom catalysts for the degradation of organic molecules using ROS. Another example of this type of reaction has been the recent work by Lís group where Fe–N–C prepared by a high-temperature gas-migration strategy exhibited outstanding peroxidase-, oxidase-, and catalase-like activities[148] whose structure was mainly determined by Cs-corrected STEM-HAADF, XANES, and EXAFS. Fe–N–C SACs reached up to 83% removal of phenol in wastewater through the production of $^{\bullet}OH$ in the presence of H_2O_2.

Other active sites different than Fe have been also reported to act as single-atom nanozymes such as cobalt, Co–N–C, which was able to catalyze the oxidation of recalcitrant organics through a stable Fenton-like reaction[31] [Fig. 7(a)]. The reaction mechanism was explained with the aid of DFT calculations, proving a higher activity of CoN_4 complexes vs CoO, graphitic nitrogen, or graphene; meanwhile, the structure was determined by SEM, TEM, and C_s-corrected STEM-HAADF [see Fig. 7(b)]. SAzymes of composition Zn–N–C have been also synthesized from metalorganic frameworks as precursors, exhibiting a remarkable peroxidase-like

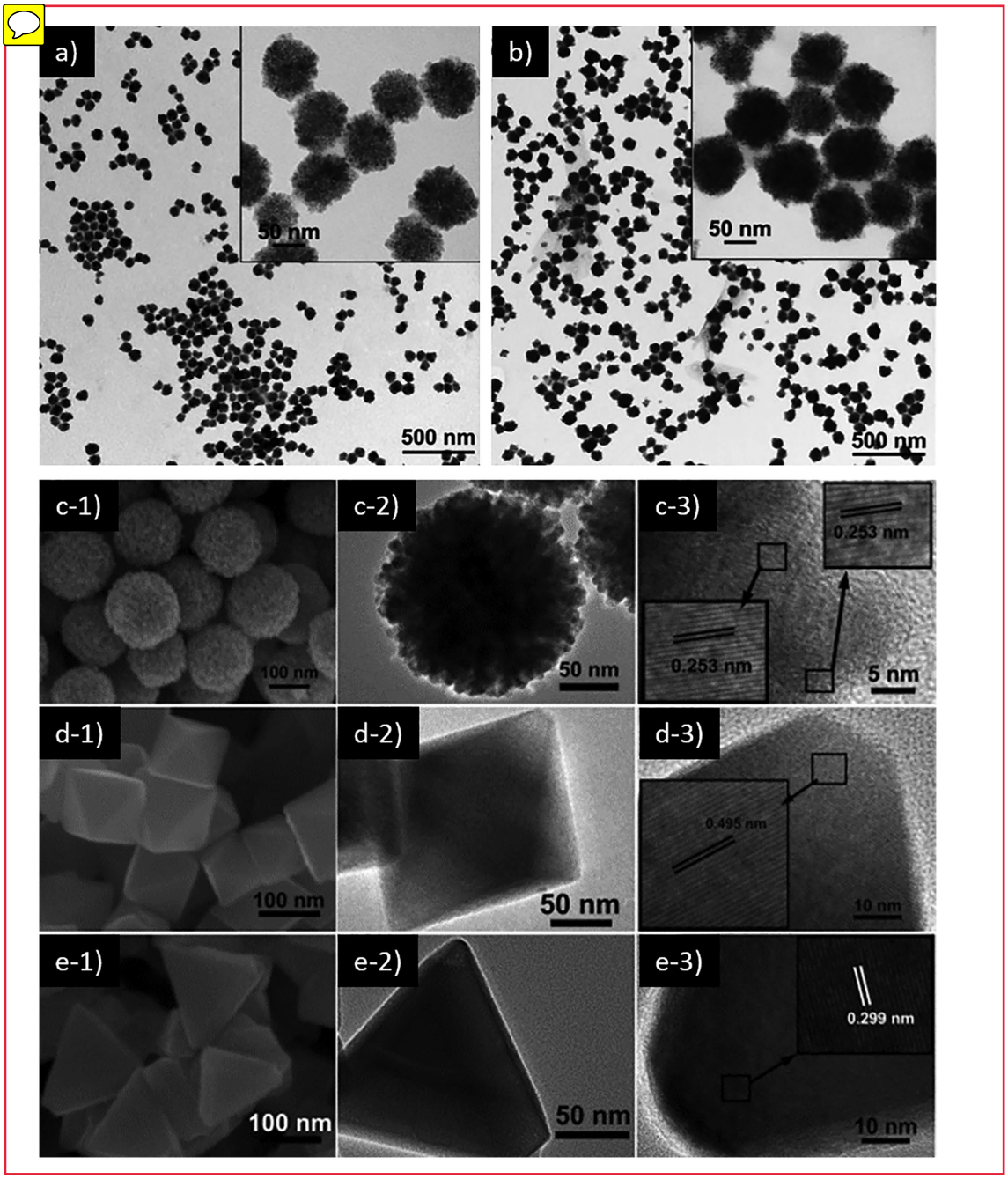

FIG. 5. (a) Low-magnification TEM image of Fe–N SAzyme. (b) Cs-corrected STEM-HAADF image observing the Fe atoms as bright spots (red circles). Adapted from Ma *et al.*, Chem. Commun. **55**, 159–162 (2019). Copyright 2019 The Royal Society of Chemistry.

activity, which can be used for antibacterial applications, as photosensitizers or in photodynamic therapy.[149]

MoS_2 is another type of support that has been used to immobilize Rh atoms for selective hydrogenation of unsaturated aldehydes to unsaturated alcohols.[150] In this work, Rh atoms were anchored to the edges of 2D MoS_2 sheets achieving 100% selectivity for the conversion of crotonaldehyde to crotyl alcohol owed to a steric confinement effect of pocketlike active sites. Theoretical DFT analyses revealed that isolated Rh atoms can be strongly anchored to Mo vacancies on the edges of the sheets forming a unique Rh–S_4

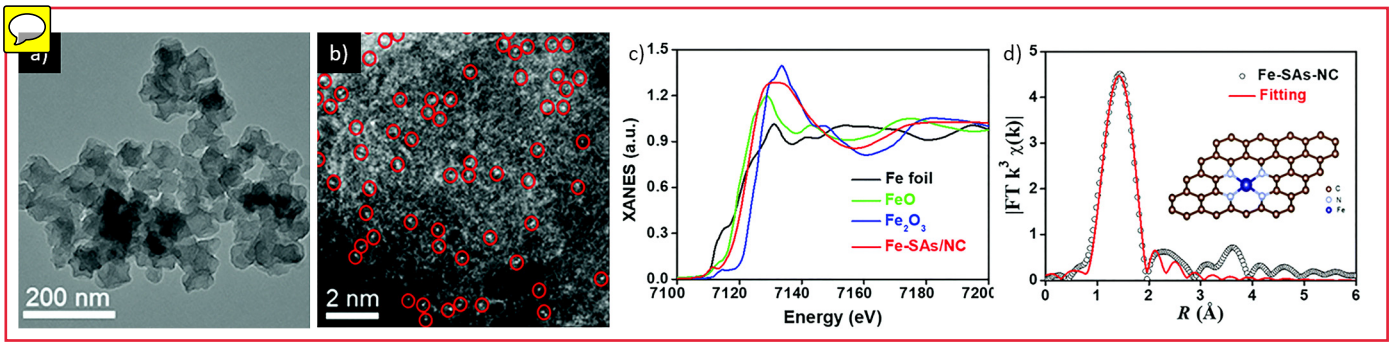

FIG. 6. (a) ACTEM image of FeN_4 on GN with red arrows indicating Fe atoms. (b) Magnified image of one of the FeN_4 complexes, marked by a dashed circle. (c) Correspondent atomistic model with Fe in purple, N in blue, and C in gray. (d) Cs-corrected STEM-HAADF, the bright spots correspond to Fe atoms. (e) Magnified Cs-corrected STEM-HAADF data with a red arrow indicating a FeN_4 site, where the chemical analysis was performed. (f) Fe and N spectra obtained from the atom marked by a red arrow.[144] Reprinted from Deng *et al.*, Sci. Adv. **1**(11), e1500462 (2015). Copyright 2015 Author(s), licensed under a Creative Commons Attribution (CC BY) license.

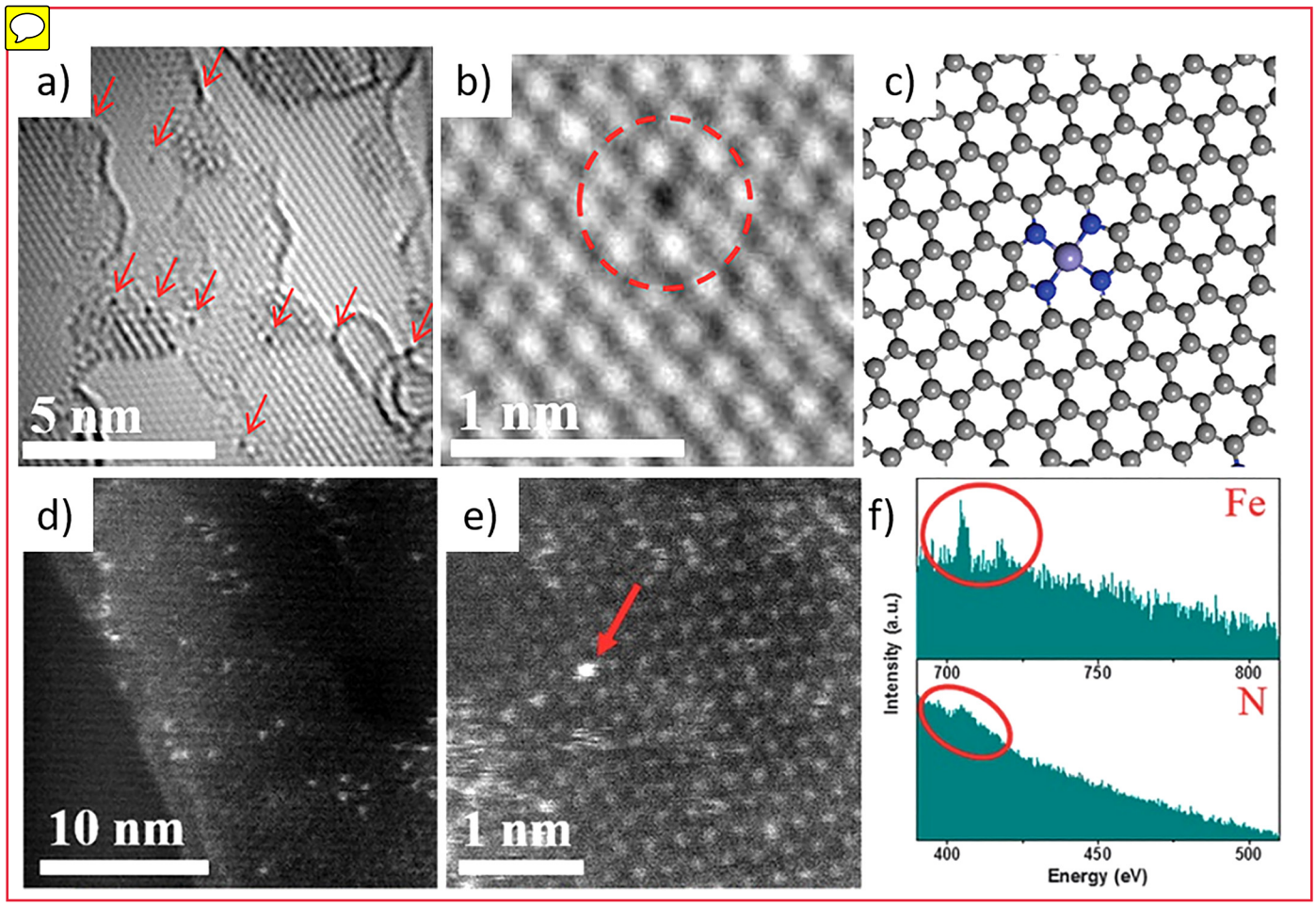

FIG. 7. (a) Proposed overall Fenton-like reaction mechanism on single-Co-atom catalyst. (b) Cs-corrected STEM-HAADF image of the Co–N–C material. In this sample, Fe and Co may coexist. Adapted from Wang *et al.*, Nat. Commun. **9**, 3334 (2018). Copyright 2018 MDPI. (c) DFT calculated model of the $Rh–S_4$ configuration. (d) C_s-corrected STEM-HAADF micrograph of the as-synthesized Rh/MoS_2 material and (e) after three cycles of selective hydrogenation reaction. Yellow arrows indicate the Rh atoms, while red dashed lines mark the edge of the sheets. Adapted from Kubaichuk *et al.*, Cells **8**(6), 598 (2019). Copyright 2019 MDPI.

complex. Figure 7(c) depicts the schematic representation of the Rh anchored to the MoS_4 sheets from a top and from a transversal view where Rh atoms (in gray) are linked to S atoms in yellow; green spheres correspond to Mo atoms while O is represented in red. Nevertheless, this was the predicted structure to investigate the real configuration authors made use of Cs-corrected STEM-HAADF to characterize at atomic level the presence of Rh atoms on the support. Low-magnification observations were performed to discard the presence of large clusters or Rh nanoparticles. Atomic visualization was carried out in what the authors claimed to be low-dose conditions (despite no values of electron dose were given) revealing the presence of isolated Rh atoms [Fig. 7(d)] indicated by yellow arrows that were decorating the MoS_2 edges (dashed red lines). It was observed that even after three reaction cycles, isolated atoms were still retained with no observation of particles or clusters [Fig. 7(e)] suggesting a strong interaction between the noble metal and the support that resulted in an excellent stability during the selective hydrogenation reaction. Further structural characterization was carried out by EXAFS, which indicated that the absence of Rh—Rh bonding in agreement with the experimental observation of isolated Rh sites. In fact, only Rh–S coordination in the first shell was observed ($R = 2.3$ Å). Moreover, the fitting results indicated that on average, Rh atoms were coordinated with four S atoms (CN = 4.4) probing the feasibility of electron microscopy, especially when it is combined with x-ray absorption techniques, to characterize at atomic level the structure of all types of nanozymes in general and single-atom nanozymes in particular.

Based on the importance that nanozymes and SAzymes will have in many of modern chemical reactions, understating their structure to correlate their physicochemical properties with the structural features is urgently needed. SAzymes exhibit outstanding structural advantages compared to nanozymes, as their active centers are simple (one atom), more controllable and definite, facilitating the understanding of the catalytic reactions that will lead into a more rational design as well as higher activity per active site. Despite its huge potential that brings together homogeneous catalysis, heterogeneous catalysis, and enzymes, there are several challenges that need to be addressed. In particular, from the characterization point of view, elucidating the real active sites and how the couple with neighbor atoms is essential in order to explore the structure–activity relationship. It is also a highly desirable dynamic observation of the nanozymes during the reaction; therefore, it is expected that with the development of *in situ* electron microscopy new insights in this aspect will be accessible.

Another aspect that needs more attention from an electron microscopy perspective is how the active sites are bonded to the support. For instance, clear atomic imaging data accompanied with spectroscopic analysis, when possible, of how Fe atoms are connected to the N atoms, which are in turn connected to the C atoms. Most of the data reported rely on the results obtained by EXAFS and XANES as well as theoretical models, but there is not yet clear evidence of whether an ordered C arrangement is present, especially for the MOF derived nanozymes and SAzymes. This is of particular interest as it is widely assumed that the surrounding of the active sites has a strong influence on the catalytic performance. Based on the current, electron microscopy capabilities in terms of spatial resolution, electron detection (sensitivity), and spectroscopic advances, this type of information is potentially available and would provide direct confirmation of the theoretical structures that are being proposed.

V. ROS QUANTIFICATION BY ELECTRON PARAMAGNETIC RESONANCE

As described in Secs. II–IV, the study of the kinetic of ROS formation by the catalytic activity of nanozymes in different conditions involves several fields of knowledge like physics, chemistry, biochemistry, and molecular biology. In fact, the study of the oxidative stress considering both measurements of ROS and the counterpart of antioxidants is determined for the understanding of the catalytic activity by nanostructures. An effective, fast, and precise determination of oxidative stress is also a central piece in biochemistry, for a better understanding of the relationship between the immune systems and related diseases.[151–155] From an experimental perspective, the above challenges require sensitive techniques to identify and quantify small concentrations of the free radicals produced in biocatalysis to unravel the different mechanisms involved in redox processes and elucidate the role played by the free radicals.

Electron paramagnetic resonance (EPR) spectroscopy is a standard technique to detect different free radicals. These species present a paramagnetic moment due to the unpaired electron that gives their high chemical reactivity. The EPR technique is based in the resonant absorption of energy by the paramagnetic moment of the free radical in the presence of a static magnetic field. To induce this resonance, the system is irradiated with microwave radiation of fixed frequency, where the most common frequency is the X-band, which is in the 9–10 GHz range. One of the remarkable characteristics of this spectroscopy is its high sensitivity, which allows us to detect less than picomolar concentrations of paramagnetic molecules. In addition, each free radical may have a characteristic EPR spectrum with a set of hyperfine parameters due to the hyperfine interaction between the unpaired electrons of the free radical with the nuclear magnetic moment of the surrounding ions. These features not only allow us to identify and quantify the free radical species but also make possible to follow the rate of the reaction.

Although some free radicals can be directly detected in biological environments by EPR, such as ascorbyl radicals, α-tocopheroxyl radical, phenoxyl radicals, nitroaromatic radical, and semiquinone radicals,[156] most of them have a very short lifetime, which makes it unable for direct measurement. This is the case of the biological relevant ROS free radicals such as $^{\bullet}O_2^-$, $^{\bullet}HO$, and $^{\bullet}HO_2$. The lifetime does not only depend on the reactivity of the free radical species in biological systems but also depend on with the level of cellular antioxidants[157] and with the interference with other reactive species present in the media. Moreover, the ROS concentration is usually very low, making the EPR detection challenging.[158]

These issues were efficiently overcome by employing molecular spin-probes, spin-labels, and spin-traps. Spin-probes are paramagnetic molecules whose EPR spectra are sensitive to the nearby environment.[156] Spin-labels are usually stable free radicals with the ability to form covalent bonds with other molecules allowing us to monitor specific reactions.[159,160] Spin-traps are diamagnetic molecules that react with short life free radicals, the adducts, resulting in a more stable free radical that can be detected by EPR.[161] In this

way, the concentration of free radicals can be directly determined from changes in the area or hyperfine parameters of spin-probe spectra and from the area of the EPR spectra in the case of spin-traps or spin-labels.[162] Although these techniques were widely used for decades to study the ROS in biochemistry, there are some limitations that have to be taken into account for its accurate measurement, for example, the toxicity of the spin-label/traps, its relative hydrophilic character, its dependence with the pH of the media, the by-reactions, and the distinct reaction rates of the different ROS species.[163] Some of the most common molecules currently used as spin-probes, spin-traps, and labels are shown in Fig. 8, as well as their EPR response in the X-band. The figure also shows the reactions with different free radicals involving the spin-trap species.

The high specificity of the spin-trap EPR technique to identify and quantify different species makes it a "gold standard" for the free radical detection. As mentioned previously, the spectrum of each adducted molecule presents a characteristic hyperfine splitting due to the interaction between the unpaired electron of the spin-trap molecule with the surrounding nuclei, resulting in a EPR spectrum that is like a "fingerprint" of the adducted radical.[161] As a general description, there are two families of spin-traps commonly used: the linear nitrones such as the N-tert-butyl-α-phenylnitrone (PBN) and α-(4-pyridyl-1-oxide)-N-tert-butylnitrone (POBN); and the pyrroline-based cyclic nitrones such as the 5,5-dimethyl-1-pyrroline-Noxide (DMPO), 5-diethoxyphosphoryl-5-methyl-1-pyrroline N-oxide (DEPMPO), and 5-(ethoxycarbonyl)-5-methyl-1-pyrroline N-oxide (EMPO), among others.[156]

Despite the fact that the BMPO and PBN are liposoluble and DMPO is soluble in water, the detection of radicals with different spin-traps at the subcellular level is really hard and requires more complex biochemical solutions, such as the use of conjugates

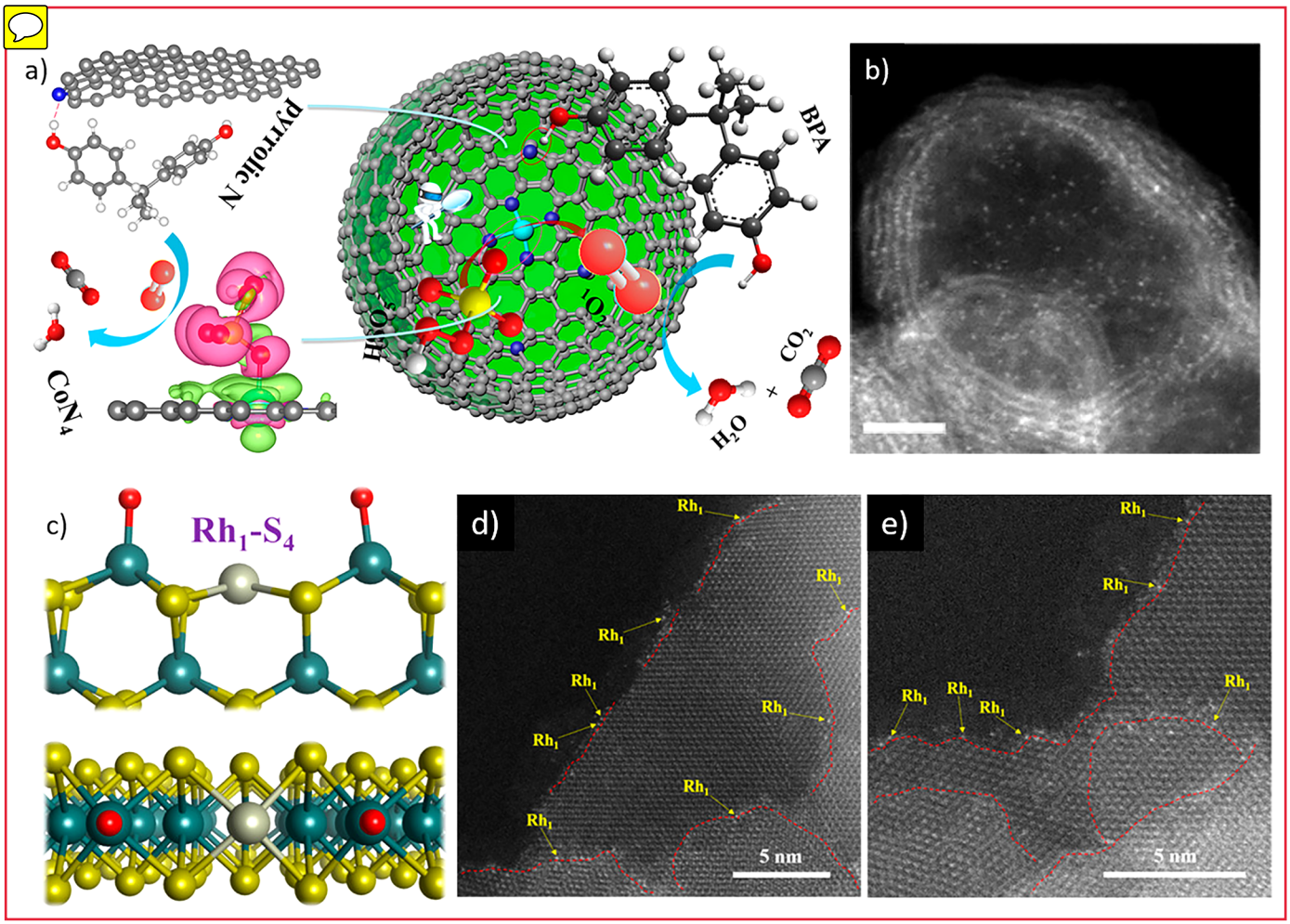

FIG. 8. EPR detection of nanozyme catalytic activity using spin-probes. Top-left panel: typical nitrone spin-probe with its characteristic EPR signal and schematic reaction with free radical R°, without EPR signal after the reaction. Top-right panel: a spin-label that conjugates a nitrone spin-probe and a protein with its characteristic EPR signal. Bottom panel: two typical spin-traps (DMPO and PBN) and their reactions with radical R° together with the characteristic EPR signal after the reaction with the free radicals ·OH, ·OOH, and ·CH

Comp: Please extract Fig. 8 from the manuscript source files (JAP21-PS-03309_art.docx) attached.
The caption is correct as it appears here.

of macromolecules to the spin-traps: the immuno-spin-traps.[164] Taking into account that the nanozyme can be functionalized to be internalized in different cellular environments, such as the lipid membrane, the lysosome, or the cytoplasm, the formation of correct immune-molecules and proper spin-traps should be selected for each case. Although the nitrone traps are relatively non-toxic at low concentration (mM) and were used in *in vivo* experiments,[165] it was reported that the toxicity is related to the hydrophobicity been the DMPO the less toxic, followed by DEPMPO and EMPO, and been more toxic the more lipid soluble BMPO and PBN.[166–170] As mentioned before, another limitation for quantification using spin-traps is the different kinetics of the free radicals. One of the most critical ROS species in biological systems is $^{\bullet}O_2^-$, and the analysis based on nitrone adduct is complex due to the relative slow kinetic of formation and a short half-life of the adducted molecule (≈50 s).[171] These lead to the underestimation of the superoxide radical, and usually the concentration of spin-traps should be increased from around 20 to 100 mM for its feasible detection.[157]

Although the EPR spin-trap technique has been used for decades, the development of new spin-traps is still a present challenge. Currently, intense research is carried out to design and fabricate novel molecules looking for an increasing rate of adduct formation, larger adduct stability, EPR spectrum allowing unambiguous ROS identification, biostability, and biocompatibility. In this way, different spin-traps were developed specifically for the $^{\bullet}O_2^-$ detection EPR such as the new cyclic DEPMPO-type nitrone the mito-DEPMPO, DEPMPO modified with a triphenyl phosphonium cation conjugated, which results to be more effective for trapping superoxide and hydroxyl than most spin-trap nitrones, or the 5-(2,2-dimethyl-1,3-propoxy cyclophosphoryl)-5-methyl-1-pyrroline N-oxide (CYPMPO).[171] Also, valuable information is obtained by using density functional theory (DFT) calculation that helps us to conduct a more systematic search for new and more efficient spin-traps. Different substitutional functional groups in nitrone spin-traps were analyzed, and from the free energies and rate constants calculation for the reactivity of $\bullet O2^-$, new families of spin-traps were proposed, such as the use of N-monoalkyl-substituted amide or an ester as attached groups on the nitrone.[163] Finally, the ability to combine spin-traps designed for the $^{\bullet}O_2^-$ detection with immuno-macromolecules can improve drastically the ability for the detection of this free radical at the subcellular level.

As already mentioned, the extreme short lifetime of most of free radicals, especially ROS, make decisive the use of appropriate spin-traps, spin-labels, and spin-probes to study and to determine the effects and effectiveness of nanozymes. This is critical for *in vitro*, *ex vivo*, and *in vivo* studies, since the low levels of ROS and complexity of biological environment increases the difficulty to perform appropriate measurements by EPR. For this reason, it is likely that future studies and clinical applications of nanozymes in theranostics will demand new systems to improve the effectiveness of *in vitro* and *in vivo* EPR detection of the ROS and new measurement protocols in order to obtain a complete characterization of the nanozymes activity and its effects.[153] These studies are critical for the development of novel nanozymes for specific functions. An interesting potential area is the design of nanozymes functionalized with spin-probes, spin-labels, or spin-traps. This class of architecture should improve the specificity in the measurement of the catalytic activity as their co-localization. As an illustrative example, Fig. 9 presents a schematic representation a functionalized ferrite

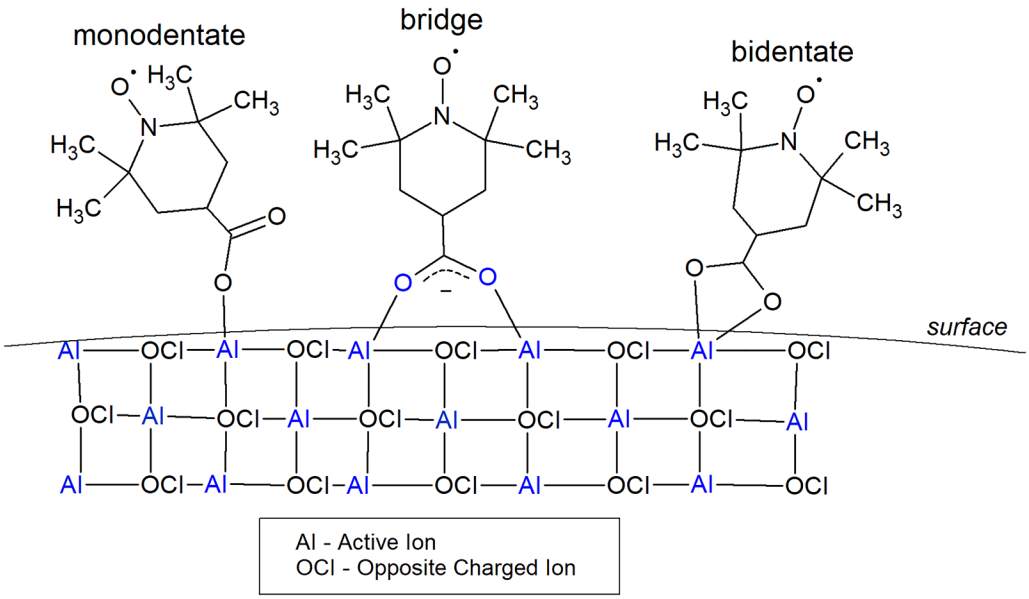

FIG. 9. Schematic representation of the proposed spin-label containing a nanoparticle with a defined crystalline structure composed by active ion (Al) and opposite-charged ion (OCl) that acts as a nanozyme functionalized with a nitrone-based spin-probe with an active carboxylic functional group that can attach with some active ions at the surface in three possible different ways.

nanoparticle that at a certain condition acts as a nanozyme functionalized with a nitrone-based spin-probe with a carboxylic functional group (carboxy-TEMPO) that has a high affinity with iron ions at the surface of the nanoparticle through different ways.

The possibility of this architecture is centered not only on the use of probes for ROS detection by EPR but also for multiple detection systems, especially with nuclear magnetic resonance (NMR/MRI) and with photoluminescence and spectrophotometry, as well as systems to detect the effects of the oxidative stress in proteins, lipids, DNA, and in the cell metabolism.[153] In addition, in the case of magnetic nanozymes, the EPR and ferromagnetic resonance (FMR) can also give information about the nanozyme itself,[172] revealing changes in the valence, phase, surface chemistry, and magnetic anisotropy during *in vivo* and *in vitro* studies.

Other points needed to improve the reliability and reproducibility of determination by EPR of the ROS and oxidative stress catalyzed by nanozymes are the improvement and development of specific protocols. In general, the protocols to measure free radicals in solutions by EPR with spin-traps and spin-probes are quite straightforward, provided that a specific probe is used at the right concentration,[171] avoiding by-products,[157] and some attention is paid to the interactions of the nanozyme and the solution elements like ions for buffer solutions. However, *in vivo* and *in vitro* measurements consist of more subtle mechanisms involving the internalization and localization of the nanozyme and of the EPR probe, by-reactions, toxicity, and oxidative stress induced by the EPR probe, among others. In a general way, the protocols for *in vitro* or *ex vivo* (tissues) measurements of ROS levels and oxidative stress[173,174] should comply with the following requirements: (i) the tissue/cell culture should be prepared for the spectral analysis, with an appropriate storage under the specific tissue/culture conditions (*in vitro* samples), particularly temperature and pH to avoid additional stress; (ii) dissolution of the tissue and cells should be performed with appropriate medium, in general, a combination of chloroform-methanol for tissues or an appropriate buffer-like saline solutions, such as PBS, taking into account the possibility of interaction among the saline solution and the nanozymes; (iii) production of homogenates, in general, with ultrasound probe or bath during short times (in general, faster than 1 min); (iv) working concentrations of the spin-trap or spin-probe added to the solution should be kept close to optimum operational ranges (for instance, about 50–10 mM for DMPO, a common spin-trap, or 5 μM for TEMPO, a common spin-probe); (v) the time scale of the experiments should match the reaction time, which depends on the nanozyme activity and the free radical specie object of study. Concerning the ROS species such as $^{\bullet}O_2^-$ and $^{\bullet}HO_2$, its indirect observation with using protocols similar to that one described previously have been performed in several biological systems, from mitochondria to human neutrophils.[175] For the EPR measurements in biological systems, a temperature control system is used, working around 310 K. For a kinetic measurement, successive measurements of the same sample or of different samples at different exposition times to the nanozyme should be performed. The amount of sample to be measured depends on the frequency of the microwave used. For the common X-band (9 GHz), a small amount of sample solution must be used due to the water absorbance, about 50–120 μl in a quartz capillary. For lower frequencies, like the L-band (1.2 GHz), a larger amount of sample could be used. However, small sensibility and resolution result from the reduction of the microwave frequency. The sample positioning and centering are also critical factors, and the use of a spin-label or a marker is very useful. The protocols for *in vivo* measuring the oxidative stress and ROS levels produced by nanozymes are not so well established as for the corresponding *in vitro* experiments, mostly because the preparation of the biological specimen requires a more complex series of steps, but also because of the need to attain a balance between the toxicity of the spin-probes and sensibility of the technique, which are related.[173] In this way, exhaustive studies with different protocols for different systems, different free radical species to be detected, and different nanozymes for *in vivo* experiments are needed. In addition, the development of new EPR probes with specificity for nanozyme studies used for *in vivo* measurements is also an interesting possibility.

Probably, the most tempting perspective regarding the detection of ROS using EPR is for clinical applications. Several experimental techniques for *in vivo* studies in animals were developed,[176,177] mainly focused on the *in vivo* oximetry (measurements of pO_2 in tissues),[178] where EPR provides accurate and reliable results with EPR imaging providing unequal spatially resolved measurements in tissues.[179] A special combination of EPR imaging (with 3D scan) and spectroscopy (with 2D scan) is specially a powerful possibility to *in situ* diagnostic or even *in vivo* studies of nanozymes' activity and the oxidative stress that it promotes. In addition, EPR is also able to give physicochemical information of physiology and biochemistry, such as the pH or viscosity, among others.[180] Its continuous development in the last 20 years promises a strong impact in diagnostics and therapies of several diseases.[179,181] However, in a widespread view, this use might expand the possibility to measure the catalytic activity of nanozymes and its biochemical effects in clinical practice. This possibility has the potential to be a real paradigm shift in the clinical uses or toxicity evaluation of nanozymes, with accurate and reliable *in situ* evaluation, allowing its application in theragnosis. The potential of this tool is exemplified in the study of melanoma B16 metastasis in mice lung, imaged by Eichhoff and Höfer.[182] Using the X-band EPR signal (see Fig. 10), the authors established that free radicals are created within the melanoma cells. Specifically, melanin is a free radical from which the presence is indicated by the black pigmentation of the melanoma, allowing a comparison between the histological study and the EPR images. A comparison between the picture of the melanoma [Fig. 10(d)] and its EPR image [Fig. 10(e)] shows that the matching is excellent. Similar conclusions can be drawn from the comparison between the lung [Fig. 10(f)], the corresponding 2D transverse EPR image [Fig. 10(g)], and the longitudinal section through 3D EPR images [Fig. 10(h)].

EPR imaging and spectroscopy clinical technique can be non-invasive depending on the frequency used. In general, low frequency systems operating in the L-band or in the range of 500 MHz are ideal due to the larger depths obtained, ranging from 10 to 80 mm, respectively.[183] The reduction in the sensibility due to the lower frequency is compensated by a larger sampling system. In addition, the use of appropriate spin-traps, spin-labels, and spin-probes together with appropriate protocols can improve drastically the sensibility of the system. EPR images for pO_2 determination can get a spatial resolution of 1.2 mm and values of 1–3 Torr

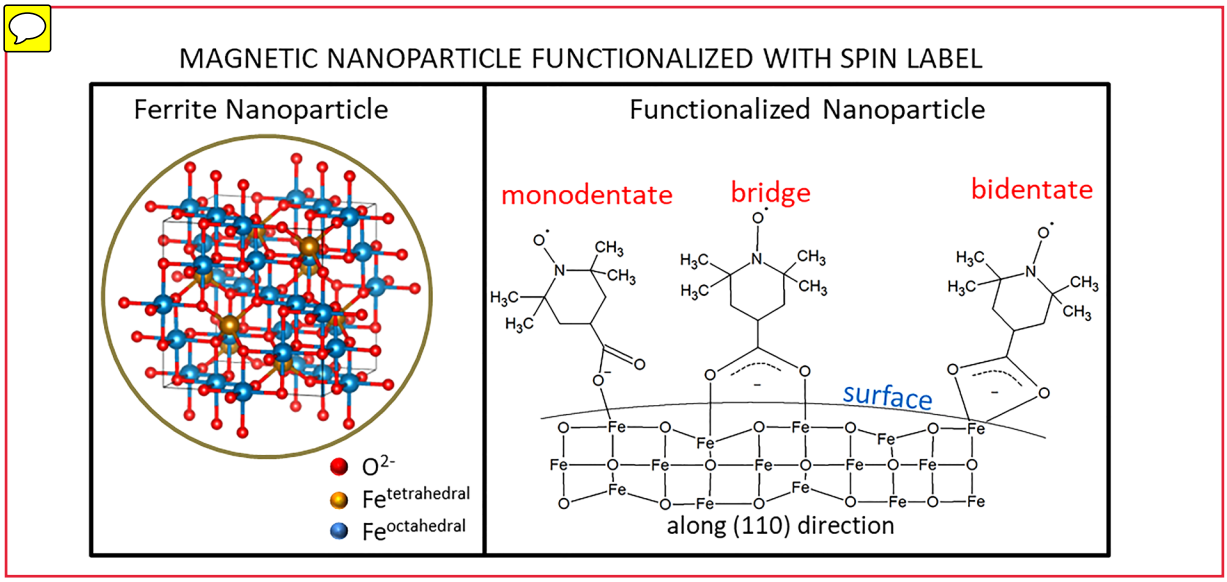

FIG. 10. (a) EPR spectrum from a freeze-dried melanoma B16 metastasis in mice lung; (b) 2D EPR image; (c) 3D EPR image; (d) picture of a fresh melanoma; (e) corresponding EPR image; (f) picture of a freeze-dried lung with metastasis; (g) 2D transverse EPR image; (h) longitudinal section through a 3D EPR image. Reprinted from Eichhoff *et al.*, Low Temp. Phys. **41**(1), 62–66 (2015).Copyright 2015 AIP Publishing LLC.

for an imaging time of 10 min.[179] The use of rapid pulsed EPR is much more effective and may reduce drastically the acquisition time, making the measurement more precise with a better resolution.[177]

In fact, the potential of *in vivo* EPR imaging increases if its ability to give information about the pharmacokinetic of the nanozymes is also taken into account. Despite several *in vivo* studies and protocols established for EPR imaging and spectroscopy regarding its use as a clinical tool in the diagnostic and evaluation of several diseases, a few works are reported until now concerning its use in the study of the pharmacokinetic and the oxidative stress promoted by the catalytic activity of nanozymes. As mentioned previously, the development of combined nanozymes and new spin-probes or spin-traps can be a very useful tool for future clinical theragnosis protocols focused on the catalytic activity of the nanostructure together with the EPR imaging and spectroscopy.

VI. THE CONCEPT OF SEQUENTIAL CATALYTIC THERAPY

Electron transfer is at the core of every single biochemical catalysis and redox chemistry process. Because biological enzymes are proteins and, therefore, electrical insulators, the first general explanation of the electron transfer between the substrate-enzyme-product complex had to wait until 1967,[184,185] when laser technology and transport measurements in biological samples at helium temperatures became technically possible.[186] Measuring the electron transfer in photosynthetic membranes down to $T = 4.4$ K allowed us to observe that electron transport became temperature-independent below 100 K, a strong indication that quantum tunneling was the main mechanism behind chlorophyll oxidation–reduction. Due to the simpler experimental approachability of photosynthetic systems, empirical and theoretical models of enzymatic electron tunneling were first applied to these systems[187,188] but swiftly extended to many eukaryotic cell pathways.[189] The same basic mechanisms of electron transfer remains invariable when considering more complex enzyme structures. Since the electron carrier function resides on the cofactor site (either a coenzyme or a prosthetic group), in biological enzymes the main role of the "protein cage" is to serve as a scaffold for the cofactors and modify some properties, for instance, to increase its solubility in water or to provide a binding and positioning site for substrates.[190]

Within the field of nanozymes applied to nanomedicine, the concept of sequential catalysis relates to the idea of sequential redox reactions triggered by changes of microenvironment.[115] The bottom line is, the distinctive characteristics of tumor microenvironments (TMEs) provide a way for designing cancer therapies based on local activation of nanozymes to produce the desired cytotoxic, antitumor agent. A recent report using glucose oxidase (GOD) grafted onto a Fe_3O_4–PPy (polypyrrole) composite nanosystem, provided a proof of concept for the sequential biocatalytic therapy.[126] Once the nanosystem enters the TME, GOD will consume the glucose usually present in large amounts, producing gluconic acid and H_2O_2 as products. The increase of the peroxide concentration will boost the Fenton reaction $H_2O_2 \rightarrow \bullet OH + OH^-$, and the resulting concentration of hydroxyl radicals (•OH) will add to the suppression of tumor cells (see Fig. 11). The PPy component aims to thermally enhance the process by an external stimulus using an infrared light source. Other similar nanosystems targeting the TME have been reported, for instance, a polydopamine (PDA)-based TME-responsive nanosystem that showed good efficacy in tumor regression by integrating catalytic glucose degradation with Fenton activity of the H_2O_2 by-product. GOD grafted onto the Fe(II)-PDA nanosystem showed good efficiency catalyzing the glucose of the

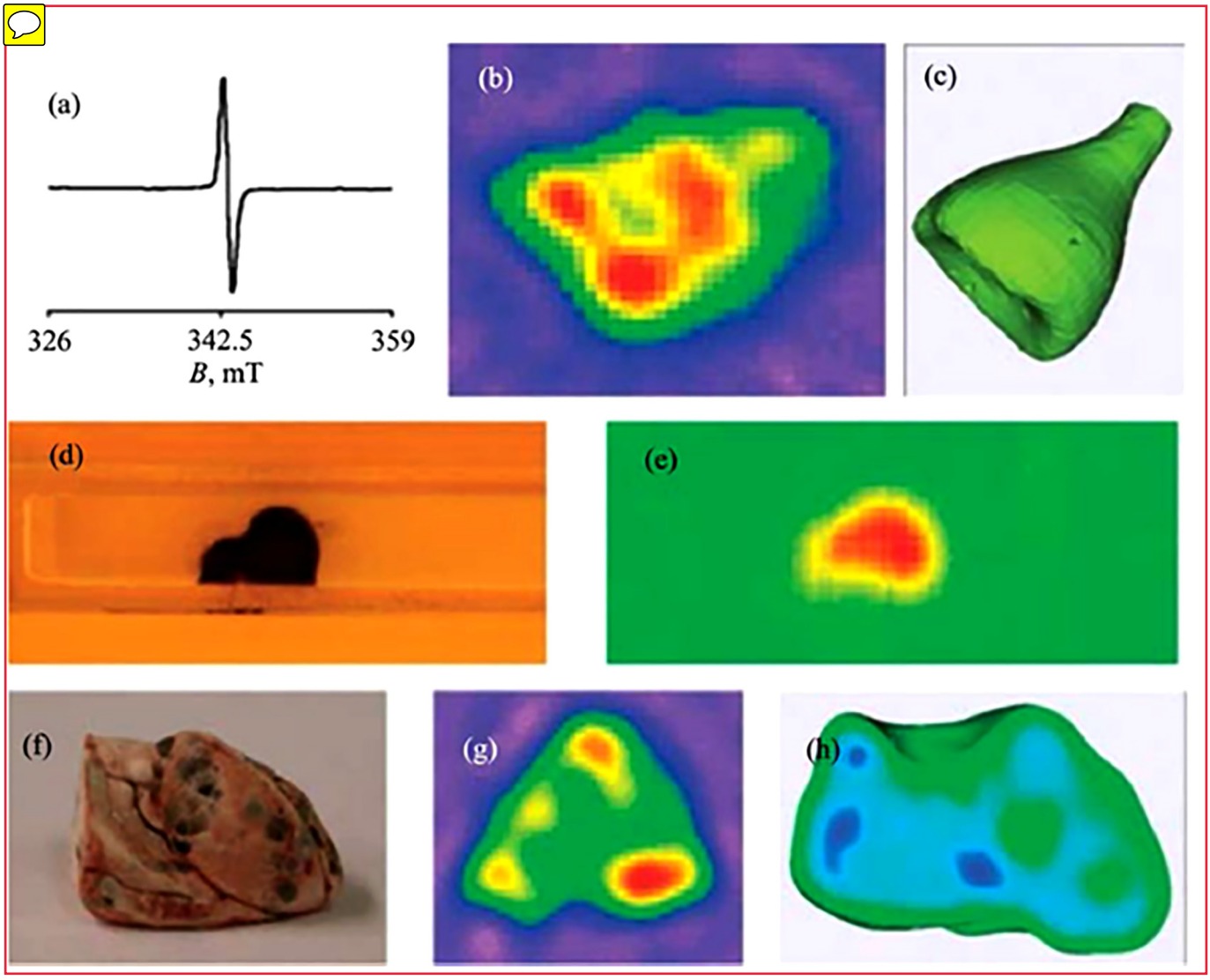

FIG. 11. (a) Scheme of the sequential catalytic process *in vivo* for tumor therapy. (b) The sequence of catalytic glucose oxidation followed by the generation of H_2O_2 to activate Fenton reaction and OH release. The process is assisted by an external infrared light source aiming photothermal enhancement of the Fe_3O_4@PPy@GOD nanosystem. Reproduced from Feng *et al.*, Adv. Mater. **31**(5), 1805919 (2019). Copyright 2019 Wiley-VCH.

TME increasing the H_2O_2 level and starting the sequential Fenton response to generate hydroxyl radicals (•OH).[115] Although these proofs of concept for sequential catalysis were performed with an external photothermal stimulus, it seems plausible that further advances in materials design could prove this type of external sources unnecessary.

VII. CHALLENGES FOR THE NEXT GENERATION OF NANOZYMES

In the field of synthetic biology, one of the key goals is to reproduce natural systems with synthetic materials keeping or improving their functions, a definition that comfortably comprises natural enzymes and their synthetic counterparts, the nanozymes. The field has, therefore, the potential to revolutionize the application of enzymology to areas even beyond biology, for instance, those critical societal needs in energy, agriculture, medicine, and industry. There are no fundamental laws of physics that could inhibit nanozymes from displaying similar or better catalytic properties than biological enzymes. However, before these levels of exquisite detail of enzymatic design and fabrication are attained, there are some big challenges related to basic properties of the nanomaterials that must be solved, some of which we hopefully have unearthed in this review. While the technologies involved in the atomic-level design of nanomaterials are already mature, it is the development of comprehensive *ab initio* models from quantum

chemistry that will show the path to where the nanofabrication should go. It is also clear that these atomistic models will need the input from many advanced characterization techniques to perform under reliable data regarding not only nanozymes' physicochemical parameters and atomic electronic configurations but also the corresponding substrate atomic configurations during the catalytic reactions under specific conditions. Thus, to attain the maturity level of enzymology with artificial nanozymes, a qualitative leap in the knowledge of molecular and atomic dynamics in nanosystems will be necessary. As a final remark, we note that applications of nanozymes to nanomedicine face additional challenges, related to the complex nature of the biochemical reactions and feedbacked cellular pathways. In this regard, the current development of new biomedical techniques including enzymatic monitoring of brain neurochemicals *in vivo*, cell vectorization of nanozymes for targeted therapies, or new EPR spin-probes for imaging provides an optimistic expectation for successful clinical uses of nanozymes in the near future.

ACKNOWLEDGMENTS

The authors acknowledge financial support from the EU-Commission (Project Nos. H2020-MSCA-RISE-2020 101007629-NESTOR and 823717-ESTEEM3), the Spanish Ministerio de Ciencia, Innovación y Universidades (Project Nos. RTC-2017-6620-1 and PID2019-106947RB-C21), the Aragon Regional Government (DGA, Project Nos. E28_20R and E13_20R), and Argentinian governmental agency ANPCyT (Project Nos. PICT-2016-0288 and PICT-2015-0883).

AUTHOR DECLARATIONS

Conflict of Interest

The authors have no conflicts to disclose.

DATA AVAILABILITY

Data sharing is not applicable to this article as no new data were created or analyzed in this study.

REFERENCES

[1]I. Ari and R. F. Yikmaz, in *Handbook of Green Economics*, edited by S. Acar and E. Yeldan (Academic Press, 2019), pp. 53–68.
[2]C. J. Clarke, W.-C. Tu, O. Levers, A. Bröhl, and J. P. Hallett, Chem. Rev. **118**(2), 747–800 (2018).
[3]J. M. Woodley, Appl. Microbiol. Biotechnol. **103**(12), 4733–4739 (2019).
[4]R. Breslow and L. E. Overman, J. Am. Chem. Soc. **92**(4), 1075–1077 (1970).
[5]I. M. Klotz, G. P. Royer, and I. S. Scarpa, Proc. Natl. Acad. Sci. U.S.A. **68**(2), 263 (1971).
[6]F. Hollfelder, A. J. Kirby, and D. S. Tawfik, J. Am. Chem. Soc. **119**(40), 9578–9579 (1997).
[7]Y. Murakami, J.-i. Kikuchi, Y. Hisaeda, and O. Hayashida, Chem. Rev. **96**(2), 721–758 (1996).
[8]L. Gao, J. Zhuang, L. Nie, J. Zhang, Y. Zhang, N. Gu, T. Wang, J. Feng, D. Yang, S. Perrett, and X. Yan, Nat. Nanotechnol. **2**(9), 577–583 (2007).
[9]L. Gao and X. Yan, in *Biological and Bio-Inspired Nanomaterials: Properties and Assembly Mechanisms*, edited by S. Perrett, A. K. Buell, and T. P. J. Knowles (Springer, Singapore, 2019), pp. 291–312.
[10]J. Mu, Y. Wang, M. Zhao, and L. Zhang, Chem. Commun. **48**(19), 2540–2542 (2012).
[11]Y. Yoshihisa, Q.-L. Zhao, M. A. Hassan, Z.-L. Wei, M. Furuichi, Y. Miyamoto, T. Kondo, and T. Shimizu, Free Radical Res. **45**(3), 326–335 (2011).
[12]A. Dhall, A. Burns, J. Dowding, S. Das, S. Seal, and W. Self, Environ. Sci. Nano **4**(8), 1742–1749 (2017).
[13]M. Nguyen, A. Robert, and B. Meunier (2021).
[14]M. Gumpelmayer, M. Nguyen, G. Molnár, A. Bousseksou, B. Meunier, and A. Robert, Angew. Chem. **130**(45), 14974–14979 (2018).
[15]B. Meunier and A. Robert, J. Phys. Chem. C **123**(46), 28513–28514 (2019).
[16]K. Chemizmu and R. Fentona, Ecol. Chem. Eng. **16**, 347–358 (2009).
[17]H. Y. Shin, T. J. Park, and M. I. Kim, J. Nanomater. **2015**, 756278 (2015).
[18]M. L. Kremer, Phys. Chem. Chem. Phys. **1**(15), 3595–3605 (1999).
[19]H. Y. Shin, T. J. Park, and M. I. Kim, J. Nanomater. **2015**, 756278 (2015).
[20]H. Xiang, W. Feng, and Y. Chen, Adv. Mater. **32**, 1905994 (2019).
[21]H. Fang, Y. Pan, W. Shan, M. Guo, Z. Nie, Y. Huang, and S. Yao, Anal. Methods **6**(15), 6073–6081 (2014).
[22]L. Zhang, Z. Qi, Y. Zou, J. Zhang, W. Xia, R. Zhang, Z. He, X. Cai, Y. Lin, S.-Z. Duan, J. Li, L. Wang, N. Lu, and Z. Tang, ACS Appl. Mater. Interfaces **11**(34), 30640–30647 (2019).
[23]Y. Zhou, C. Liu, Y. Yu, M. Yin, J. Sun, J. Huang, N. Chen, H. Wang, C. Fan, and H. Song, Adv. Mater. **32**(45), 2003708 (2020).
[24]N. Alizadeh and A. Salimi, J. Nanobiotechnol. **19**(1), 26 (2021).
[25]A. Gallo-Cordova, J. J. Castro, E. L. Winkler, E. Lima, R. D. Zysler, M. d, P. Morales, J. G. Ovejero, and D. A. Streitwieser, J. Cleaner Prod. **308**, 127385 (2021).
[26]M. Li, H. Zhang, Y. Hou, X. Wang, C. Xue, W. Li, K. Cai, Y. Zhao, and Z. Luo, Nanoscale Horiz. **5**(2), 202–217 (2020).
[27]R. Singh and S. Singh, Mater. Today Proc. **10**, 25–31 (2019).
[28]Y. Yin, L. Shi, W. Li, X. Li, H. Wu, Z. Ao, W. Tian, S. Liu, S. Wang, and H. Sun, Environ. Sci. Technol. **53**(19), 11391–11400 (2019).
[29]L. Jiao, H. Yan, Y. Wu, W. Gu, C. Zhu, D. Du, and Y. Lin, Angew. Chem. Int. Ed. **59**(7), 2565–2576 (2020).
[30]L. Jiao, H. Yan, Y. Wu, W. Gu, C. Zhu, D. Du, and Y. Lin, Angew. Chem. **59**, 2565 (2019).
[31]Z. Wang, Y. Zhang, E. Ju, Z. Liu, F. Cao, Z. Chen, J. Ren, and X. Qu, Nat. Commun. **9**, 3334 (2018).
[32]L.-H. Frahm and D. Pfannkuche, J. Chem. Theory Comput. **15**(4), 2154–2165 (2019).
[33]A. Ardèvol and C. Rovira, J. Am. Chem. Soc. **137**(24), 7528–7547 (2015).
[34]R. P. Mason and D. Ganini, Free Radical Biol. Med. **131**, 318–331 (2019).
[35]X. Shen, W. Liu, X. Gao, Z. Lu, X. Wu, and X. Gao, J. Am. Chem. Soc. **137**(50), 15882–15891 (2015).
[36]Y. Liu, H. Wu, M. Li, J. J. Yin, and Z. Nie, Nanoscale **6**(20), 11904–11910 (2014).
[37]Y. Liu, Y. Cheng, H. Zhang, M. Zhou, Y. Yu, S. Lin, B. Jiang, X. Zhao, L. Miao, C.-W. Wei, Q. Liu, Y.-W. Lin, Y. Du, C. J. Butch, and H. Wei, Sci. Adv. **6**(29), eabb2695 (2020).
[38]J. Wei, X. Chen, S. Shi, S. Mo, and N. Zheng, Nanoscale **7**(45), 19018–19026 (2015).
[39]G. Fang, W. Li, X. Shen, J. M. Perez-Aguilar, Y. Chong, X. Gao, Z. Chai, C. Chen, C. Ge, and R. Zhou, Nat. Commun. **9**(1), 129 (2018).
[40]W. He, Y. T. Zhou, W. G. Wamer, X. Hu, X. Wu, Z. Zheng, M. D. Boudreau, and J. J. Yin, Biomaterials **34**(3), 765–773 (2013).
[41]H. Tombuloglu, Y. Slimani, G. Tombuloglu, M. Almessiere, A. Baykal, I. Ercan, and H. Sozeri, Environ. Nanotechnol. Monit. Manage. **11**, 100223 (2019).
[42]Y. Zhang, Z. Zhou, F. Wen, J. Tan, T. Peng, B. Luo, H. Wang, and S. Yin, Sens. Actuators B **275**, 155–162 (2018).
[43]F. Xia, Q. Shi, and Z. Nan, Surf. Interfaces **24**, 101109 (2021).
[44]Y. W. Fan, W. B. Shi, X. D. Zhang, and Y. M. Huang, J. Mater. Chem. A **2**(8), 2482–2486 (2014).

[45]X. Yin, P. Liu, X. Xu, J. Pan, X. Li, and X. Niu, Sens. Actuators B **328**, 129033 (2021).
[46]W. Lu, J. Chen, L. Kong, F. Zhu, Z. Feng, and J. Zhan, Sens. Actuators B **333**, 129560 (2021).
[47]Y. Huang, Z. Liu, C. Liu, E. Ju, Y. Zhang, J. Ren, and X. Qu, Angew Chem. Int. Ed. Engl. **55**(23), 6646–6650 (2016).
[48]C. Feng, Y. Yan, Z. Zhang, K. Xu, and Z. Wang, Org. Biomol. Chem. **12**(27), 4837–4840 (2014).
[49]T. M. Chen, X. M. Tian, L. Huang, J. Xiao, and G. W. Yang, Nanoscale **9**(40), 15673–15684 (2017).
[50]R. André, F. Natálio, M. Humanes, J. Leppin, K. Heinze, R. Wever, H.-C. Schröder, W. E. G. Müller, and W. Tremel, Adv. Funct. Mater. **21**(3), 501–509 (2011).
[51]A. A. Vernekar, D. Sinha, S. Srivastava, P. U. Paramasivam, P. D'Silva, and G. Mugesh, Nat. Commun. **5**(1), 5301 (2014).
[52]D. Wang, H. Wu, C. Wang, L. Gu, H. Chen, D. Jana, L. Feng, J. Liu, X. Wang, P. Xu, Z. Guo, Q. Chen, and Y. Zhao, Angew. Chem. Int. Ed. **60**(6), 3001–3007 (2021).
[53]L. Huang, D.-W. Sun, H. Pu, Q. Wei, L. Luo, and J. Wang, Sens. Actuators B **290**, 573–580 (2019).
[54]X. Wu, T. Chen, J. Wang, and G. Yang, J. Mater. Chem. B **6**(1), 105–111 (2018).
[55]S. Li, L. Zhang, Y. Jiang, S. Zhu, X. Lv, Z. Duan, and H. Wang, Nanoscale **9**(41), 16005–16011 (2017).
[56]Y. Shi, J. Huang, J. N. Wang, P. Su, and Y. Yang, Talanta **143**, 457–463 (2015).
[57]Z. Wang, Y. Zhang, E. Ju, Z. Liu, F. Cao, Z. Chen, J. Ren, and X. Qu, Nat. Commun. **9**(1), 3334 (2018).
[58]M. Diez-Castellnou, F. Mancin, and P. Scrimin, J. Am. Chem. Soc. **136**(4), 1158–1161 (2014).
[59]P. Pengo, L. Baltzer, L. Pasquato, and P. Scrimin, Angew. Chem. Int. Ed. **46**(3), 400–404 (2007).
[60]B. Halliwell and J. M. Gutteridge, *Free Radicals in Biology and Medicine* (Oxford University Press, 2015).
[61]B. Halliwell, Plant Physiol. **141**(2), 312–322 (2006).
[62]J. F. Turrens, J. Physiol. **552**(2), 335–344 (2003).
[63]Y. J. Taverne, D. Merkus, A. J. Bogers, B. Halliwell, D. J. Duncker, and T. W. Lyons, Bioessays **40**(3), 1700158 (2018).
[64]R. Gerschman, D. L. Gilbert, S. W. Nye, P. Dwyer, and W. O. Fenn, Science **119**(3097), 623–626 (1954).
[65]M. C. W. Oswald, N. Garnham, S. T. Sweeney, and M. Landgraf, FEBS Lett. **592**(5), 679–691 (2018).
[66]P. D. Ray, B.-W. Huang, and Y. Tsuji, Cell. Signalling **24**(5), 981–990 (2012).
[67]J. M. Gutteridge and B. Halliwell, *Free Radicals in Biology and Medicine* (Clarendon Press, 1985).
[68]I. Fridovich, J. Biol. Chem. **272**(30), 18515–18517 (1997).
[69]L. A. Johnson and L. A. Hug, Free Radical Biol. Med. **140**, 93–102 (2019).
[70]L. M. Sayre, M. A. Smith, and G. Perry, Curr. Med. Chem. **8**(7), 721–738 (2001).
[71]K. Fukui, J. Clin. Biochem. Nutr. **59**(3), 155–159 (2016).
[72]E. F. Armstrong, Nature **131**(3311), 535–537 (1933).
[73]C. M. Heckmann and F. Paradisi, ChemCatChem **12**(24), 6082–6102 (2020).
[74]A. L. Lehninger, *Biochemistry: The Molecular Basis of Cell Structure and Function*, 2nd ed. (Worth Publishers, New York, 1975).
[75]X. Wang, X. J. Gao, L. Qin, C. Wang, L. Song, Y.-N. Zhou, G. Zhu, W. Cao, S. Lin, and L. Zhou, Nat. Commun. **10**(1), 1–8 (2019).
[76]C. Lamberti, S. Bordiga, F. Bonino, C. Prestipino, G. Berlier, L. Capello, F. D'Acapito, F. L. i Xamena, and A. Zecchina, Phys. Chem. Chem. Phys. **5**(20), 4502–4509 (2003).
[77]Y. Wang, G. Jia, X. Cui, X. Zhao, Q. Zhang, L. Gu, L. Zheng, L. H. Li, Q. Wu, and D. J. Singh, Chem **7**(2), 436–449 (2021).
[78]T. Kandemir, F. Girgsdies, T. C. Hansen, K. D. Liss, I. Kasatkin, E. L. Kunkes, G. Wowsnick, N. Jacobsen, R. Schlögl, and M. Behrens, Angew. Chem. Int. Ed. **52**(19), 5166–5170 (2013).
[79]M. Chen, H. Zhou, X. Liu, T. Yuan, W. Wang, C. Zhao, Y. Zhao, F. Zhou, X. Wang, and Z. Xue, Small **16**(31), 2002343 (2020).
[80]P. D. Boyer and E. G. Krebs, *The Enzymes* (Academic Press, 1986).
[81]L. Stryer, *Biochemistry* (WH Freeman and Company, 1995).
[82]M. Yan, B. Yuan, Y. Xie, S. Cheng, H. Huang, W. Zhang, J. Chen, and C. Cao, Postharvest Biol. Technol. **166**, 111230 (2020).
[83]S. Abbet, U. Heiz, H. Häkkinen, and U. Landman, Phys. Rev. Lett. **86**(26), 5950–5953 (2001).
[84]E. Z. Eisenmesser, O. Millet, W. Labeikovsky, D. M. Korzhnev, M. Wolf-Watz, D. A. Bosco, J. J. Skalicky, L. E. Kay, and D. Kern, Nature **438**(7064), 117–121 (2005).
[85]Q. Fu, H. Saltsburg, and M. Flytzani-Stephanopoulos, Science **301**(5635), 935–938 (2003).
[86]R. Bashyam and P. Zelenay, *Materials for Sustainable Energy* (Eprld Scientific, 2010), pp. 247–250.
[87]B. Qiao, A. Wang, X. Yang, L. F. Allard, Z. Jiang, Y. Cui, J. Liu, J. Li, and T. Zhang, Nat. Chem. **3**(8), 634–641 (2011).
[88]M. S. Kim, J. Lee, H. S. Kim, A. Cho, K. H. Shim, T. N. Le, S. S. A. An, J. W. Han, M. I. Kim, and J. Lee, Adv. Funct. Mater. **30**(1), 1905410 (2020).
[89]W. Song, B. Zhao, C. Wang, Y. Ozaki, and X. Lu, J. Mater. Chem. B **7**(6), 850–875 (2019).
[90]Y. Wu, Y. Chen, Y. Li, J. Huang, H. Yu, and Z. Wang, Sens. Actuators B **270**, 443–451 (2018).
[91]Y. Zhou, B. Liu, R. Yang, and J. Liu, Bioconjugate Chem. **28**(12), 2903–2909 (2017).
[92]Z. Zhang, X. Zhang, B. Liu, and J. Liu, J. Am. Chem. Soc. **139**(15), 5412–5419 (2017).
[93]Q. Wang, H. Wei, Z. Zhang, E. Wang, and S. Dong, TrAC Trends Anal. Chem. **105**, 218–224 (2018).
[94]Z. Dai, J. Guo, J. Xu, C. Liu, Z. Gao, and Y.-Y. Song, Anal. Chem. **92**(14), 10033–10041 (2020).
[95]I. I. Vlasova, Molecules **23**(10), 2561 (2018).
[96]N. Wang, L. Zhu, D. Wang, M. Wang, Z. Lin, and H. Tang, Ultrason. Sonochem. **17**(3), 526–533 (2010).
[97]J. Flemmig and J. Arnhold, J. Inorg. Biochem. **104**(7), 759–764 (2010).
[98]A. P. Chapman, T. Mocatta, S. Shiva, A. Seidel, B. Chen, I. Khalilova, M. E. Paumann-Page, G. L. Jameson, C. Winterbourn, and A. J. Kettle, J. Biol. Chem. **288**(9), 6465–6477 (2013).
[99]I. I. Vlasova, J. Arnhold, A. N. Osipov, and O. M. Panasenko, Biochemistry **71**(6), 667–677 (2006).
[100]D. Eleftheriadou, D. Kesidou, F. Moura, E. Felli, and W. Song, Small **16**(43), 1907308 (2020).
[101]R. Cao-Milán, S. Gopalakrishnan, L. D. He, R. Huang, L.-S. Wang, L. Castellanos, D. C. Luther, R. F. Landis, J. M. V. Makabenta, C.-H. Li, X. Zhang, F. Scaletti, R. W. Vachet, and V. M. Rotello, Chem **6**(5), 1113–1124 (2020).
[102]W. Li, G.-C. Fan, F. Gao, Y. Cui, W. Wang, and X. Luo, Biosens. Bioelectron. **127**, 64–71 (2019).
[103]J. F. Kornecki, D. Carballares, P. W. Tardioli, R. C. Rodrigues, Á Berenguer-Murcia, A. R. Alcántara, and R. Fernandez-Lafuente, Catal. Sci. Technol. **10**(17), 5740–5771 (2020).
[104]C. Lu, L. Tang, F. Gao, Y. Li, J. Liu, and J. Zheng, Biosens. Bioelectron. **187**, 113327 (2021).
[105]R. Yu, R. Wang, Z. Wang, Q. Zhu, and Z. Dai, Analyst **146**(4), 1127–1141 (2021).
[106]E. Katz, A. Riklin, V. Heleg-Shabtai, I. Willner, and A. F. Bückmann, Anal. Chim. Acta **385**(1), 45–58 (1999).
[107]Y. Ouyang, Y. Biniuri, M. Fadeev, P. Zhang, R. Carmieli, M. Vázquez-González, and I. Willner, J. Am. Chem. Soc. **143**(30), 11510–11519 (2021).
[108]P. D. Bank, National Science Foundation (DBI-1832184), the U.S. Department of Energy (DE-SC0019749), 1971.

[109]M. Garcia-Viloca, J. Gao, M. Karplus, and D. G. Truhlar, Science **303**(5655), 186–195 (2004).
[110]A. Prah, E. Franciskovic, J. Mavri, and J. Stare, ACS Catal. **9**(2), 1231–1240 (2019).
[111]S. J. Benkovic and S. Hammes-Schiffer, Science **301**(5637), 1196–1202 (2003).
[112]Z. Y. Song, H. L. Fu, R. Baumgartner, L. Y. Zhu, K. C. Shih, Y. C. Xia, X. T. Zheng, L. C. Yin, C. Chipot, Y. Lin, and J. J. Cheng, Nat. Commun. **10**, 7 (2019).
[113]W. R. Cannon, S. F. Singleton, and S. J. Benkovic, Nat. Struct. Biol. **3**(10), 821–833 (1996).
[114]L. Gao, M. Liu, G. Ma, Y. Wang, L. Zhao, Q. Yuan, F. Gao, R. Liu, J. Zhai, Z. Chai, Y. Zhao, and X. Gao, ACS Nano **9**, 10979–10990 (2015).
[115]X. Wang, M. Li, Y. Hou, Y. Li, X. Yao, C. Xue, Y. Fei, Y. Xiang, K. Cai, Y. Zhao, and Z. Luo, Adv. Funct. Mater. **30**(40), 2000229 (2020).
[116]F. Branda, B. Silvestri, A. Costantini, and G. Luciani, J. Sol-Gel Sci. Technol. **73**(1), 54–61 (2015).
[117]L. Tao, M. Qiao, R. Jin, Y. Li, Z. Xiao, Y. Wang, N. Zhang, C. Xie, Q. He, and D. Jiang, Angew. Chem. Int. Ed. **58**(4), 1019–1024 (2019).
[118]Y. Lv, M. Ma, Y. Huang, and Y. Xia, Chem. Eur. J. **25**, 954–960 (2019).
[119]Q. Liu, H. Li, Q. Zhao, R. Zhu, Y. Yang, Q. Jia, B. Bian, and L. Zhuo, Mater. Sci. Eng. C **41**, 142–151 (2014).
[120]J. Sun, C. Li, Y. Qi, S. Guo, and X. Liang, Sensors **16**, 584 (2016).
[121]M. Raineri, E. L. Winkler, T. E. Torres, M. Vasquez Mansilla, M. S. Nadal, R. D. Zysler, and E. Lima, Nanoscale **11**(39), 18393–18406 (2019).
[122]R. Zeng, Z. Luo, L. Zhang, and D. Tang, Anal. Chem. **90**, 12299–12306 (2018).
[123]S. Sloan-Dennison, S. Laing, N. C. Shand, D. Graham, and K. Faulds, Analyst **142**, 2484–2490 (2017).
[124]S. Wen, X. Ma, H. Liu, G. Chen, H. Wang, G. Deng, Y. Zhang, W. Song, B. Zhao, and Y. Ozaki, Anal. Chem. **92**, 11763–11770 (2020).
[125]X. Wang, L. Qin, M. Zhou, Z. Lou, and H. Wei, Anal. Chem. **90**, 11696–11702 (2018).
[126]W. Feng, X. Han, R. Wang, X. Gao, P. Hu, W. Yue, Y. Chen, and J. Shi, Adv. Mater. **31**(5), 1805919 (2019).
[127]B. Xu, H. Wang, W. Wang, L. Gao, S. Li, X. Pan, H. Wang, H. Yang, X. Meng, Q. Wu, L. Zheng, S. Chen, X. Shi, K. Fan, X. Yan, and H. Liu, Angew. Chem. Int. Ed. **131**, 4965–4970 (2019).
[128]S. Ray, R. Biswas, R. Banerjee, and P. Biswas, Nanoscale Adv. **2**, 734–745 (2020).
[129]L. Qin, Y. Hu, and H. Wei, in *Nanozymology*, edited by X. Yan (Springer, 2020), pp. 79–101.
[130]F. L. Deepak, A. Mayoral, and R. Arenal, *Advanced Transmission Electron Microscopy: Applications to Nanomaterials* (Springer International Publishing, 2015).
[131]D. Jo, Y. Zhang, J. H. Lee, A. Mayoral, J. Shin, N. Y. Kang, Y. K. Park, and S. B. Hong, Angew. Chem. Int. Ed. **133**, 6001–6005 (2021).
[132]O. Krivanek, N. Dellby, A. J. Spence, R. A. Camps, and L. M. Brown, in *Proceedings of the EMAG 1997, Cambridge, UK* (The Royal Society Publishing, 1997), pp. 35–49.
[133]A. Mayoral, R. M. Hall, R. Jackowska, and J. E. Readman, Angew. Chem. Int. Ed. **55**, 16127–16131 (2016).
[134]L. Gao, J. Zhuang, L. Nie, J. Zhang, Y. Zhang, N. Gu, T. Wang, J. Feng, D. Yang, S. Perrett, and X. Yan, Nat. Nanotechnol. **2**, 577–583 (2007).
[135]L. Huang, J. Chen, L. Gan, J. Wang, and S. Dong, Sci. Adv. **5**, eaav5490 (2019).
[136]S. Liu, F. Lu, R. Xing, and J. J. Zhu, Chem. Eur. J. **17**, 620–625 (2011).
[137]L. Jiao, H. Yan, Y. Wu, W. Gu, C. Zhu, D. Du, and Y. Lin, Angew. Chem. Int. Ed. **59**, 2565–2576 (2020).
[138]A. A. Vernekar, D. Sinha, S. Srivastava, P. U. Paramasivam, P. D'Silva, and G. Mugesh, Nat. Commun. **5**, 5301 (2014).
[139]H. Ding, B. Hu, B. Zhang, H. Zhang, X. Yan, G. Nie, and M. Liang, Nano Res. **14**, 570–583 (2021).
[140]Y. Sang, Y. Huang, W. Li, J. Ren, and X. Qu, Chem. Eur. J. **24**, 7259–7263 (2018).
[141]H. J. Sun, N. Gao, K. Dong, J. S. Ren, and X. G. Qu, ACS Nano **8**(6), 6202–6210 (2014).
[142]H. Zhang, X. F. Lu, Z. P. Wu, and X. W. D. Lou, ACS Cent. Sci. **6**, 1288–1301 (2020).
[143]W. Ma, J. Mao, X. Yang, C. Pan, W. Chen, M. Wang, P. Yu, and L. Mao, Chem. Commun. **55**, 159–162 (2019).
[144]D. Deng, X. Chen, L. Yu, X. Wu, Q. Liu, Y. Liu, H. Yang, H. Tian, Y. Hu, P. Du, R. Si, J. Wang, X. Cui, H. Li, J. Xiao, T. Xu, J. Deng, F. Yang, P. N. Duchesne, P. Zhang, J. Zhou, L. Sun, J. Li, X. n. Pan, and X. Bao, Sci. Adv. **1**, e1500462 (2015).
[145]A. M. Klibanov and E. D. Morris, Enzyme Microbiol. Technol. **3**, 119–122 (1981).
[146]T. Mester and M. Tien, Int. Biodeterior. Biodegradation **46**, 51–59 (2000).
[147]F. He, L. Mi, Y. Shen, T. Mori, S. Liu, and Y. Zhang, ACS Appl. Mater. Interfaces **10**, 35327–35333 (2018).
[148]C. Zhao, C. Xiong, X. Liu, M. Qiao, Z. Li, T. Yuan, J. Wang, Y. Qu, X. Wang, F. Zhou, Q. Xu, S. Wang, M. Chen, W. Wang, Y. Li, T. Yao, Y. Wu, and Y. Li, Chem. Commun. **55**, 2285–2288 (2019).
[149]S. Wang, L. Shang, L. Li, Y. Yu, C. Chi, K. Wang, J. Zhang, R. Shi, H. Shen, G. I. N. Waterhouse, S. Liu, J. Tian, T. Zhang, and H. Liu, Adv. Mater. **28**, 8379–8387 (2016).
[150]Y. Lou, Y. Zheng, X. Li, N. Ta, J. Xu, Y. Nie, K. Cho, and J. Liu, J. Am. Chem. Soc. **141**, 19289–19295 (2019).
[151]M. Pohanka, Folia Microbiol. **58**(6), 503–513 (2013).
[152]A. Ceriello, R. Testa , and S. Genovese, Nutr. Metab. Cardiovas. Dis. **26**(4), 285–292 (2016).
[153]M. Katerji, M. Filippova, and P. Duerksen-Hughes, Oxid. Med. Cell. Longevity **2019**, 1279250 (2019).
[154]U. Asmat, K. Abad, and K. Ismail, Saudi Pharm. J. **24**(5), 547–553 (2016).
[155]H. van der Vaart, D. S. Postma, W. Timens, and N. H. Ten Hacken, Thorax **59**(8), 713–721 (2004).
[156]E. G. Bagryanskaya, O. A. Krumkacheva, M. V. Fedin, and S. R. Marque, Methods Enzymol. **563**, 365–396 (2015).
[157]S. I. Dikalov and D. G. Harrison, Antioxid. Redox Signaling **20**(2), 372–382 (2014).
[158]E. Cadenas and K. J. A. Davies, Free Radical Biol. Med. **29**(3), 222–230 (2000).
[159]C. M. Arroyo and M. Kohno, Free Radical Res. Commun. **14**(2), 145–155 (1991).
[160]A. J. Carmichael, L. Steel-Goodwin, B. Gray, and C. M. Arroyo, Free Radical Res. Commun. **19**(Suppl 1), S1-16 (1993).
[161]R. Haywood, *Encyclopedia of Biophysics* (Springer, Berlin, 2013), pp. 2447–2453.
[162]A. C. Moreno Maldonado, E. L. Winkler, M. Raineri, A. Toro Córdova, L. M. Rodríguez, H. E. Troiani, M. L. Mojica Pisciotti, M. V. Mansilla, D. Tobia, M. S. Nadal, T. E. Torres, E. De Biasi, C. A. Ramos, G. F. Goya, R. D. Zysler, and E. Lima, J. Phys. Chem. C **123**(33), 20617–20627 (2019).
[163]F. A. Villamena, S. Xia, J. K. Merle, R. Lauricella, B. Tuccio, C. M. Hadad, and J. L. Zweier, J. Am. Chem. Soc. **129**(26), 8177–8191 (2007).
[164]R. P. Mason, Redox Biol. **8**, 422–429 (2016).
[165]S. Yue Qian, M. B. Kadiiska, Q. Guo, and R. P. Mason, Free Radical Biol. Med. **38**(1), 125–135 (2005).
[166]N. Khan, C. M. Wilmot, G. M. Rosen, E. Demidenko, J. Sun, J. Joseph, J. O'Hara, B. Kalyanaraman, and H. M. Swartz, Free Radical Biol. Med. **34**(11), 1473–1481 (2003).
[167]G. Gosset, J.-L. Clément, M. Culcasi, A. Rockenbauer, and S. Pietri, Bioorg. Med. Chem. **19**(7), 2218–2230 (2011).
[168]R. F. Haseloff, K. Mertsch, E. Rohde, I. Baeger, I. A. Grigor'ev, and I. E. Blasig, FEBS Lett. **418**(1–2), 73–75 (1997).
[169]N. Rohr-Udilova, K. Stolze, B. Marian, and H. Nohl, Bioorg. Med. Chem. Lett. **16**(3), 541–546 (2006).

[170]C. L. Hawkins and M. J. Davies, Biochim. Biophys. Acta Gen. Subj. **1840**(2), 708–721 (2014).
[171]K. Saito, M. Takahashi, M. Kamibayashi, T. Ozawa, and M. Kohno, Free Radical Res. **43**(7), 668–676 (2009).
[172]C. Zhang, W. Bu, D. Ni, S. Zhang, Q. Li, Z. Yao, J. Zhang, H. Yao, Z. Wang, and J. Shi, Angew. Chem. Int. Ed. **55**(6), 2101–2106 (2016).
[173]D. J. Brackett, G. Wallis, M. F. Wilson, and P. B. McCay, *Free Radical and Antioxidant Protocols* (Springer, 1998), pp. 15–25.
[174]S. Lohan, S. Ahlberg, A. Mensch, D. Höppe, M. Giulbudagian, M. Calderón, S. Grether-Beck, J. Krutmann, J. Lademann, and M. Meinke, Cell Biochem. Biophys. **75**(3), 359–367 (2017).
[175]S. Suzen, H. Gurer-Orhan, and L. Saso, Molecules **22**(1), 181 (2017).
[176]G. He, R. A. Shankar, M. Chzhan, A. Samouilov, P. Kuppusamy, and J. L. Zweier, Proc. Natl. Acad. Sci. U.S.A. **96**(8), 4586–4591 (1999).
[177]S. S. Eaton, Y. Shi, L. Woodcock, L. A. Buchanan, J. McPeak, R. W. Quine, G. A. Rinard, B. Epel, H. J. Halpern, and G. R. Eaton, J. Magn. Reson. **280**, 140–148 (2017).
[178]B. Epel, G. Redler, and H. J. Halpern, in *Oxygen Transport to Tissue XXXVI* (Springer-Verlag, New York, 2014), pp. 113–119.
[179]B. Epel, M. Kotecha, and H. J. Halpern, J. Magn. Reson. **280**, 149–157 (2017).
[180]H. M. Swartz, N. Khan, J. Buckey, R. Comi, L. Gould, O. Grinberg, A. Hartford, H. Hopf, H. Hou, E. Hug, A. Iwasaki, P. Lesniewski, I. Salikhov, and T. Walczak, NMR Biomed. **17**(5), 335–351 (2004).
[181]S. Liu, G. S. Timmins, H. Shi, C. M. Gasparovic, and K. J. Liu, NMR Biomed. **17**(5), 327–334 (2004).
[182]U. Eichhoff and P. Höfer, Low Temp. Phys. **41**(1), 62–66 (2015).
[183]P. Kuppusamy and J. L. Zweier, NMR Biomed. **17**(5), 226–239 (2004).
[184]D. DeVault and B. Chance, Biophys. J. **6**(6), 825–847 (1966).
[185]D. O. N. Devault, J. H. Parkes, and B. Chance, Nature **215**(5101), 642–644 (1967).
[186]J. McFadden and J. Al-Khalili, Proc. R. Soc. A **474**(2220) (2018), 20180674.
[187]J. Hopfield, Proc. Natl. Acad. Sci. U.S.A. **71**(9), 3640–3644 (1974).
[188]D. V. Der Vartanian and J. LeGall, Biochim. Biophys. Acta **346**(1), 79–99 (1974).
[189]D. N. Beratan, J. N. Onuchic, and J. Hopfield, J. Chem. Phys. **86**(8), 4488–4498 (1987).
[190]V. R. Kaila, M. I. Verkhovsky, and M. Wikstrom, Chem. Rev. **110**(12), 7062–7081 (2010).